Probing Organic Glasses at Low Temperature with Variable Time Scale Optical Dephasing Measurements

L. R. NARASIMHAN, K. A. LITTAU, DEE WILLIAM PACK, Y. S. BAI, A. ELSCHNER, and M. D. FAYER*

Department of Chemistry, Stanford University, Stanford, California 94305

Received October 11, 1989 (Revised Manuscript Received February 12, 1990)

Contents

I. Introduction

Amorphous materials at low temperature have markedly different physical and thermal properties from crystals.[1] For example, the specific heats of crystals obey the Debye T^3 law at low temperatures[2] and the thermal conductivity also follows the same T^3 temperature dependence.[3] Many of these properties can be calculated because crystals have long-range spatial and orientational order.[4] Twenty years ago, specific heat measurements on disordered materials revealed significant deviations from the Debye law at approximately 1 K.[5-8] Measurements of thermal conductivity[5,9] and dielectric response[10,11] also deviated from crystalline behavior. These observations showed that the dynamics of ordered and disordered systems must be fundamentally different. Although ordered crystals are commonly found in nature, many other naturally occurring complex systems, such as proteins, are inherently disordered.[12] Furthermore, many artificial materials, such as polymeric solids and amorphous semiconductors, are glasses. Therefore, understanding the microscopic behavior of the glassy state has been and continues to be[13-15] an important problem in chemistry, physics, and materials science.

Glasses are systems in which there is no translational or rotational order. More important, unlike a crystal, a glass is not in thermodynamic equilibrium. At low temperature, the equilibrium state of a substance like ethanol is crystalline. A glass is formed by rapid cooling, which traps the material in the glassy state. Thermodynamically the material should be a crystal, but kinetics prevent the system from finding the global potential minimum; i.e., the kinetics at low temperature make the time scale for crystallization essentially infinitely long. Dynamics in simple crystals involve fast fluctuations about an equilibrium structure.[16] In contrast, glass dynamics involve fast fluctuations about local structures as well as time evolution of the nonequilibrium local structures themselves.[17] Glass dynamics can occur through essentially all time scales from femtoseconds, to kiloseconds, and perhaps longer.[18-20]

Many concepts that are useful in describing dynamics in crystals cannot be extended to the amorphous state, e.g., translational symmetry, which gives rise to phonon bands and fast phonon fluctuations, providing a separation of time scales for a variety of processes.[21] In crystals at low temperatures, only the acoustic phonons are thermally excited. The phonon dispersion is well described by the Debye density of states,[4,16] and this means that the distribution of fluctuation rates is known. A glass also has modes that are equivalent to a crystal's phonons. Even at low temperatures, however, there is a major contribution to the dynamical properties of glasses from the evolution of local structures, and it is these "extra" dynamics that make glasses fundamentally different from crystals.

The anomalous heat capacities found in glasses show a term linear in temperature which is not present in crystals. This is true in such diverse substances as silicates and ceramics as well as poly(methyl methacrylate) and Lexan polymers.[5-8,22] In addition, heat capacities are time dependent; the heat capacity increases as time increases.[18,19,23,24] Thermal conductivity, which varies as T^3 in crystals, varies as T^2.[9] The phonon mean free path in a glass is substantially less than in the corresponding crystal, and a variation in the velocity of sound with temperature is seen in amorphous systems.[25] Many theoretical models have been developed to account for the various observations. The models invoke defect-induced scattering,[26] localized electronic states,[27] and defect and particle diffusion[28] to explain aspects of the observed behaviors. The two-level-system (TLS) model proposed independently by Anderson et al.[29] and Phillips[30] has been the most widely used, and it is frequently the point of departure in discussing the properties of low-temperature glasses.

The TLS model postulates that, in an amorphous material, some atoms or molecules (or groups of atoms or molecules) can reside in not just one but two potential minima of the local structure potential surface (Figure 1). Each side of the double-well potential represents a distinct local structure of the glass. This is a simplified representation of what is almost certainly a complex multidimensional potential surface. At low temperatures, transitions from one side of the double well to the other represent changes in the local structure. Transitions occur by phonon-assisted tunneling. To model the complex distribution of local structures and transition rates, the TLS model states that there

0009-2665/90/0790-0439$09.50/0

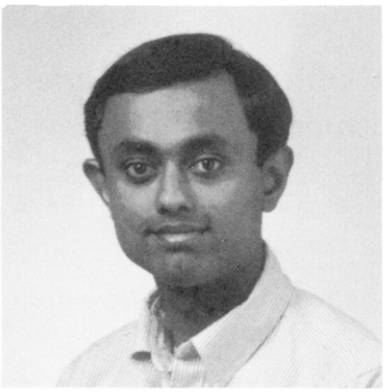

Ravi Narasimhan received a B.S. degree (Chemistry) in 1985 from the University of California, Berkeley. He is presently at Stanford University, working toward a Ph.D. in Chemistry.

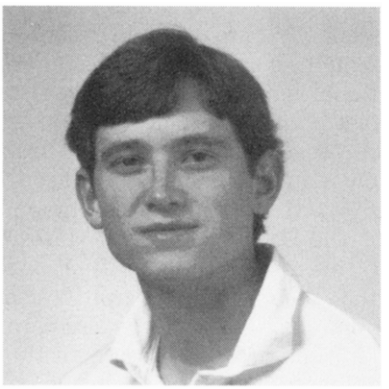

Karl Littau received a B.S. degree (Chemistry) in 1985 from the University of California, Berkeley. He is presently at Stanford University, working toward a Ph.D. in Chemistry.

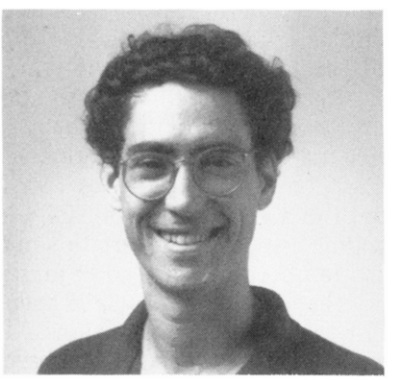

Dee William Pack received a B.S. (Chemistry) from the University of Virginia in 1982. He worked with Prof. D. S. McClure at Princeton University, receiving his Ph.D. in 1987. Until 1989, he worked as a postdoctoral fellow with Prof. Michael Fayer at Stanford University. He is currently a member of the technical staff in the Chemistry and Physics Laboratory, The Aerospace Corporation, in Los Angeles.

Yu Sheng Bai received a Ph.D. in Physics from Harvard University in 1987. He is presently a postdoctoral fellow at Stanford University.

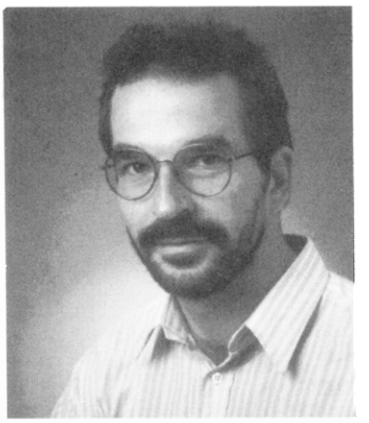

Andreas Elschner obtained a Dr. rer. nat. in 1988 from the Fachbereich Physikalische Chemie in Marburg, FRG, where he worked with Prof. H. Bässler. He returned to Marburg after a year as a postdoctoral fellow with Prof. Michael Fayer at Stanford. He is presently an Assistant Researcher in Prof. Bässler's group.

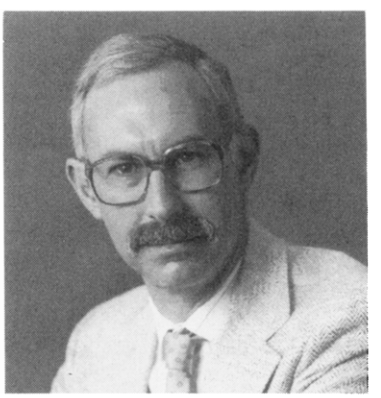

Michael Fayer obtained his Ph.D. from the University of California, Berkeley, in 1974. He then joined the faculty at Stanford University and has been a full Professor there since 1984. His research interests include intermolecular interactions and dynamics in condensed-matter systems investigated with ultrafast nonlinear optical methods, conventional spectroscopy, and theory.

is a very broad distribution of double-well asymmetries (energy differences between the two sides) and a very broad distribution of tunneling parameters (matrix elements that couple the two sides of the double well and are responsible for transitions). At low temperatures, one only considers the lowest levels in each of the two potential wells. Because of the broad distributions of asymmetries and tunneling parameters, there is a broad temperature-dependent range of time scales for transitions between the two wells (structural evolution of the glass). The TLS model accounts for many of the experimental observations that have been made on glasses. A linear term in the specific heat can be obtained by considering the excitation of the TLS from the low-energy side of the double well to the high-energy side if the TLS energy splittings are distributed uniformly for energies (kT) spanned by the measurements.[29,30] The TLS can also absorb phonons, decreasing their mean free path relative to crystals.[7] The observation of saturation in ultrasonic attenuation measurements is consistent with the TLS model since,

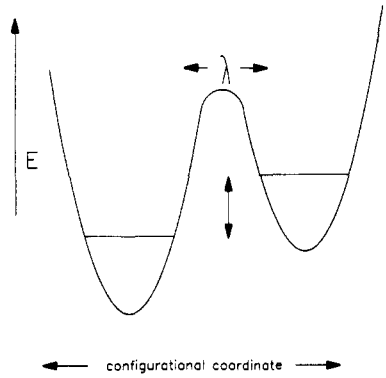

Figure 1. Schematic of a two-level system (TLS). Each well represents some particular configuration of the glassy system with energy E and a tunneling parameter λ. It is a collection of these modes, not present in crystals, with a wide distribution of E and λ that give rise to the anomalous thermal properties of glasses at low temperatures. The double arrow emphasizes the asymmetry between the two wells.

at sufficient input energy, the populations of the TLS having a particular energy (the acoustic frequency) will be equalized and no further absorption can take place.[5] A broad distribution of transition rates between the sides of the double wells (broad distribution of tunneling parameters) is suggested by the time dependence of the specific heat measurements. The temperature dependence of optical spectroscopic experiments on glasses has also been explained by the two-level-system model.[15,31] In spite of the success of the TLS model, other models are also capable of explaining the observations[32] and have not been ruled out.

Optical dephasing measurements (optical line-narrowing experiments) have developed into powerful tools for investigating the nature of glass dynamics and elucidating various phenomena of scientific[33] and potential technological importance.[34] By embedding low concentrations of chromophores in a glassy host, it is possible to examine optical dephasing (time domain) or optical line shapes (frequency domain) to obtain information on the dynamics of the glass. Fluctuations of the glassy medium couple to the energy levels of the optical centers because of intermolecular interactions. This causes the chromophore energy levels to fluctuate, inducing optical dephasing (line broadening). Because of the wide variety of local environments surrounding the optical centers in a glass, the optical spectrum is inhomogeneously broadened. Therefore it is not possible to directly measure the molecular line shape (frequently called the homogeneous line shape), which contains information on dynamics. This has resulted in the application of many line-narrowing methods, all of which have in common the ability to eliminate the inhomogeneous broadening from an optical spectrum and to reveal the underlying line shape which is a result of the dynamics of the medium.[35-39]

The frequency-domain methods, hole burning and fluorescence line narrowing, have been extensively applied over the past 15 years to study dynamical properties such as TLS densities of states,[15,40,41] kinetics of the burning process,[42-44] and chromophore–glass coupling mechanisms.[44] In addition, many groups have applied hole burning to storing information in both sequential and associative memories.[45-47] These results have been the subject of excellent recent reviews by Macfarlane and Shelby,[13] Rebane and Rebane,[14] and Hayes, Jankowiak, and Small.[15] These articles contain comprehensive summaries of the many systems that have been studied, a survey of experimental techniques and apparatus, and an outline of some of the theoretical ideas used to interpret the data.

In this article, we focus on recent theoretical and experimental developments on a different aspect of the problem: Extracting dynamical information, such as fluctuation rate distributions, from disordered systems. These studies exploit the intrinsic time scales to which different experiments are sensitive as a way to probe and quantify the time evolution of these materials. Shelby and Macfarlane showed the importance of examining complex systems with line-narrowing measurements on different time scales. Their elegant series of experiments on the Pr^{3+}:CaF_2 crystal showed that photon echo experiments gave a substantially narrower line width (Fourier transform of the echo decay) than optical hole-burning measurements.[48] In addition, they did time-dependent hole burning in which they varied the time between burning and reading and observed that the hole width increased as the time delay increased. Their emphasis was on explaining the mechanism of the time-dependent broadening. The F nuclear spins couple to the Pr^{3+} electronic states through the hyperfine interaction. There is a distribution of spin flip rates that depends on the separation between the fluorine and praseodymium ions. The short-time hole-burning measurements were sensitive only to rapidly flipping fluorine ions. The slower flip rates affected the intermediate- and long-time measurements. A subsequent detailed analysis of the hole width as a function of time yielded the spin flip rate distribution.[49]

While Shelby and Macfarlane examined a complex crystal, the Haarer group demonstrated time-dependent hole widths in a glass.[20,50] They burned a hole on a minute time scale and observed its width over several days. They observed hole width changes of over 30%. Unlike the spin flip mechanism in the Pr^{3+}:CaF_2 crystal, they attributed the width change to the structural evolution of the nonequilibrium glassy system.

The emphasis in this article is on the dynamics of "spectral diffusion". The theory discussed differs from past treatments which relied on line-shape formalisms (two-time dipole correlation functions) appropriate for crystals but not glasses.[51] Treating the different optical line-narrowing techniques as variants of four-wave mixing experiments[52,53] results in the development of a four-time correlation function description of the experiments which supersedes the more traditional two-time correlation function approach to line-narrowing spectroscopy.[53-55] The four-time correlation function appropriate for each experiment, when averaged over the parameters of the glass, describes the experimental observables for the characteristic time scale of the experiment and therefore allows information on dynamics and intermolecular interactions to be extracted.

Of particular interest are two experiments, the photon echo,[37,56,57] which is in the time domain (the optical analogue of the magnetic resonance spin echo), and nonphotochemical optical hole burning, which is in the frequency domain.[13-15,35-39,57-59] Until recently, it was believed that these two methods gave the same information about the dynamics in glasses and other com-

plex systems. Careful experiments and theoretical analysis have shown, however, that the echo is sensitive to fast fluctuations in a medium (homogeneous dephasing) while hole burning is sensitive to both fast and slow dynamics (homogeneous dephasing and spectral diffusion).[60,61] In fact, these experiments are complementary, and the application of both techniques (as well as other methods such as stimulated photon echoes[62] and accumulated photon echoes[63]) are providing a detailed view of the dynamics in low-temperature glasses which is not obtainable with previous approaches.

The results of dephasing measurements on a variety of glassy systems are presented. The shape of the photon echo decay yields information on the fluctuation rate distribution for fast rates as well as the specific nature of the chromophore–glass coupling.[54,64-66] The temperature dependence of the dephasing time follows a power law at low temperatures as has been observed previously in hole-burning experiments.[67] This is shown to be consistent with a TLS description of glasses, and it provides information on the distribution of energy levels of the glass. At higher temperatures the temperature-dependent optical dephasing rates reveal an exponentially activated process.[54,65,66] Although this type of behavior is seen in crystals, the mechanism in a polymeric glass is fundamentally different.

Dephasing rates measured by hole burning are substantially faster than those measured by photon echoes on the same system.[54,65] The increased hole line widths (dephasing rates) are a result of the long time scale dynamics in the glasses which cause spectral diffusion. The theoretical basis for hole broadening as the time scale of the measurement is increased is given along with experimental data which allows the form of the fluctuation rate distribution for slow rates to be extracted.[54,63,68]

Strong support for the validity of the TLS model is obtained through a temperature-cycled hole-burning experiment in which it is shown that the local potential surfaces in the medium do not evolve on a time scale exceeding that of the experiment (1000 s) at very low temperatures.[68] These fixed-potential surfaces are the basis of the TLS model. Heat capacity and other measurements can be explained not only by the TLS model but also with models based on particle and/or defect diffusion.[26-28,32] The temperature-cycling experiments can be explained quantitatively with no adjustable parameters with the TLS model but cannot be described in terms of a diffusion model. Finally, it is shown that a comparison of echo and hole-burning results can provide information on dynamics in the solvation shells that surround ionic chromophores.[65,69]

II. Theory

Spectral line shapes measure the interaction between an optical center and its environment. The optical line width of an isolated molecule in the gas phase is related to its excited-state lifetime. The line width of a molecule in a crystal is influenced by interactions with the phonons (lattice modes).[16,21] The time-dependent perturbations of the energy levels of a molecule by the phonon heat bath increase the line width beyond the minimum lifetime broadened width. In a glass, the constantly changing local structures influence the shape and can further increase the width. At very low temperatures, the structural fluctuations overwhelm the phonon-induced line broadening and are responsible for broadening beyond the minimum width.[70]

An absorption spectrum of a molecule embedded in an ideal crystal would show a single sharp zero phonon line whose width is influenced by interactions with phonons and a phonon sideband. Studying this homogeneous width as a function of temperature, for example, can reveal whether acoustic or optical phonons are responsible for the broadening and what the coupling strengths are.[16,21,59,71,72] In a classic experiment by Sturge and McCumber, the direct absorption spectrum approach was used to study the Cr^{3+} transition responsible for the red color in ruby crystals.[72] In the vast majority of materials it is not possible to produce a crystal in which the true homogeneous optical line width can be observed. Defects and strains will cause variations in lattice site energies. A low-temperature spectrum of a crystal will, in general, have a major contribution from inhomogeneous broadening. The static variations in the transition energies of the optical centers because of local differences in environment are considerably larger at low temperatures than the homogeneous line width. Thus it is not possible to obtain dynamical information from an absorption spectrum. To observe the homogeneous line width and obtain useful dynamical information, it is necessary to remove the inhomogeneous line broadening. The problem in a glass is even more extreme because the enormous variety of local solvent configurations generate very large inhomogeneous broadening. While guest molecules in mixed molecular crystals have inhomogeneous widths of several cm^{-1},[13,59,71] chromophores in a glass have inhomogeneous widths of several hundred cm^{-1}.[13,59] The homogeneously broadened lines of interest are typically small fractions of a wavenumber.[13,54,56,59,65,71]

A number of optical line-narrowing methods have been developed to remove the inhomogeneous broadening. Among these are hole burning,[36,38] fluorescence line narrowing,[35,39] accumulated grating echoes,[63] stimulated photon echoes,[71,89] and photon echoes.[37,56] The photon echo and the stimulated photon echo are the direct optical analogues of the magnetic resonance spin echo and stimulated spin echo.[73-75] In magnetic resonance it is known that the spin echo measures the homogeneous dephasing time (T_2)[73] and that the stimulated echo can have additional contributions to the dephasing time from spectral diffusion occurring on time scales slower than T_2.[74,75] Until recently, hole burning and fluorescence line narrowing have been the line-narrowing techniques applied to the study of glasses. Various workers have defined the observables of these techniques as the homogeneous line width.[76,77] Each technique, however, is sensitive to processes over a different range of time scales and, in general, will yield different line widths.[20,48,60,65] The line-narrowing experiments have been treated as if they are absorption experiments using optical absorption formalisms. The line-narrowed line shape was taken to be related to the Fourier transform of the two-time transition dipole moment correlation function[51]

$$I(\omega_L - \omega_0) \propto \int dt \exp[i(\omega_L - \omega_0)t]\langle \mu(t)\mu^*(0)\rangle \quad (1)$$

where μ is the transition dipole moment operator and $\omega_L - \omega_0$ is the detuning of the laser frequency from the

transition frequency of the chromophores. The correlation function is

$$\langle \mu(t)\mu^*(0)\rangle = \left\langle \exp\left[-i\int_0^t \Delta(t')\,dt'\right]\right\rangle \qquad (2)$$

where the Δ represents both the time-dependent and time-independent transition energies of the chromophores. The different energies are caused by static and dynamic interactions of the chromophores with their environments. The two-time dipole correlation function describes the free induction decay experiment, and the frequency-domain line-narrowing experiments were considered to be the Fourier transform of a free induction decay. The two-time dipole correlation function is sensitive to both static and dynamic line-broadening mechanisms. In inhomogeneously broadened systems such as glasses and most crystals, it will be totally dominated by the inhomogeneous contributions to the line width. It was assumed in the theoretical treatments the two-time correlation function could describe the optical line width with the inhomogeneous contribution removed. However, it is insufficient to describe actual line-narrowing experiments such as hole burning which are performed on glasses. In fact, the two-time correlation function description of experiments has been misleading. It indicated that all of the line-narrowing experiments measured the same observable, the homogeneous line. It caused the fundamentally distinct nature of different experiments, i.e., the characteristic time scale associated with each experiment, to be absent from the theoretical treatments. Using the correct description of the different experiments makes it possible to obtain information on the broad distribution of rates of dynamical processes in complex systems.

The proper analysis of the experiments is made possible through the recent theoretical work of Mukamel[52] and Mukamel and Loring.[53] They have developed a novel formalism that is generally applicable to four-wave mixing experiments both in the time and frequency domains. It permits determination of the form of the correlation function to be used in describing a given experiment. For example, they used the formalism to examine stimulated Raman scattering experiments in liquids and showed that they were not line-narrowing experiments.[78] The formalism has been applied by Berg et al.[54] and recently extended by Bai and Fayer[55] to the specific problem of dephasing in low-temperature glasses. They analyzed a specific model of glass dynamics for various experimental observables and subsequently developed a method for extracting dynamical information from experiment without a specific model. The more general treatment[55] can be used to extract dynamical information from systems other than glasses.[49,55]

Each line-narrowing technique can be regarded as a specific case of a four-wave mixing experiment in which three input beams induce and subsequently interfere with a polarization in a medium to generate a fourth (signal) beam. The frequency-domain experiments have specific time-domain analogues obtained through Fourier transforms. The differences between the techniques are reduced to the timing between the pulses in the time-domain description. It has also been shown[54,55] that all of the line-narrowing experiments currently being performed on glasses are describable in terms of correlation functions that are variants of the stimulated echo four-time correlation function

$$C(\tau,T_w,\tau) = \left\langle \exp\left[i\left(\int_{T_w+\tau}^{T_w+2\tau}\Delta(t')\,dt' - \int_0^{\tau}\Delta(t')\,dt'\right)\right]\right\rangle \qquad (3)$$

In a stimulated echo, three pulses are applied at times 0, τ, and $\tau + T_w$. A fourth pulse, the signal, emerges at time $2\tau + T_w$. The correlation function is usually specified by the time intervals between the pulses, i.e., τ, T_w, and τ. The detailed analysis shows that the difference among the various line-narrowing experiments is the duration of the interval T_w, which has a major influence on the observables in the experiments.

First consider the photon echo experiment. It is the limit of a stimulated echo experiment with $T_w = 0$. The second and third pulses in the sequence are time coincident. The correlation function is

$$C(\tau,0,\tau) = \left\langle \exp\left[i\left(\int_{\tau}^{2\tau}\Delta(t')\,dt' - \int_0^{\tau}\Delta(t')\,dt'\right)\right]\right\rangle \qquad (4)$$

In a photon echo experiment,[37,56] chromophores are coherently excited by a pulse of light. The ground and excited states of all of the molecules are placed in coherent superposition states. There is a well-defined phase relationship among the superposition states. The phase relationships are lost because of inhomogeneous broadening of the optical line and dynamic interactions with the environment (homogeneous dephasing). A given time τ later, another pulse effectively changes the sign of the phase factor associated with each superposition state. This starts a rephasing process. At time 2τ, the inhomogeneous dephasing is rephased, and emission of the photon echo pulse of light occurs. The initial polarization in the sample induced by the first pulse is not completely recovered because of random fluctuations which cause homogeneous dephasing. Only the static inhomogeneous dephasing is rephased at 2τ. Therefore the signal is a measure of the extent of homogeneous dephasing that has occurred between $t = 0$ and 2τ. Inhomogeneous broadening is eliminated by the echo pulse sequence. The polarization in the sample decays as the separation between the two excitation pulses is increased. If the homogeneous line shape is Lorentzian, the polarization decays as $e^{-2\tau/T_2}$ and the signal intensity decays as $e^{-4\tau/T_2}$,[37,56] where T_2 is the homogeneous or transverse dephasing time. In addition to the dynamics-induced dephasing, population decay also contributes to the coherence loss. The pure dephasing time T_2^* can be obtained through

$$1/T_2 = 1/T_2^* + 1/2T_1 \qquad (5)$$

where T_1 is the excited-state lifetime.

The photon echo experiment can be understood qualitatively by a classical analogy. Consider a collection of oscillators that are all excited at $t = 0$. If they all have the same frequency, they will oscillate in phase. If there is a spread in the oscillator frequencies (inhomogeneous broadening), the oscillators will soon get out of phase (free induction decay). The higher frequency oscillators will be ahead in phase and the lower frequency oscillators will be behind in phase. The second pulse in the echo sequence at τ acts on the oscillators, causing the ones that are ahead in pulse an amount θ to suddenly be behind θ. Those that were behind are suddenly an equal amount ahead. Since they continue

to oscillate at their original individual frequencies, the ones that are now behind catch up, and the ones that are now ahead fall back. At 2τ, they are all in phase again. Therefore the inhomogeneous dephasing has been rephased. Homogeneous dephasing in this analogy is random fluctuations about the initial frequency of each oscillator. These fluctuations are not rephased and at 2τ, the oscillators are not perfectly rephased, even though the inhomogeneous dephasing has been eliminated. The elimination of inhomogeneous dephasing by the photon echo can be seen mathematically by inspecting eq 4. If there is only static inhomogeneous dephasing, the energies, Δ, in the right integral are identical with those in the left integral. Therefore the two integrals are identical, and when subtracted, they cancel. The correlation function does not decay from inhomogeneous dephasing. If there are also random fluctuations in the energies, the fluctuations will not be identical in the two time intervals. The integrals will not cancel, and the correlation function will decay.

In a stimulated echo.[62,71,89] a pulse excites the chromophores as before but at time τ, the second pulse is split into two pulses separated by the interval T_w. The echo appears as a fourth pulse. The stimulated photon echo is sensitive to homogeneous dephasing during the interval τ between the first and second pulses and between the third and echo pulses. It is also sensitive to frequency fluctuations (spectral diffusion) which occur on the slower time scale T_w.[71,89]

Nonphotochemical hole burning is a frequency-domain line-narrowing experiment.[13-15] In a hole-burning experiment, a narrow-band laser excites a narrow transition frequency subset of the chromophores in the inhomogeneous line. Optical excitation of molecules causes transient perturbations of the intermolecular interactions with the environment. A small fraction of the excited molecules experience a structural rearrangement of the local glass structure. This induces a large permanent shift in the absorption frequency of a subset of the excited molecules. This is in contrast to photochemical hole burning, where the chromophore undergoes a photochemical change.[14] A spectrum bracketing the point of excitation will show reduced absorption, the hole. Only molecules that were excited by the laser can contribute to the hole, these being ones either initially on resonance with the laser, or ones that had fluctuations in energy during the hole-burning period that brought them into resonance with the laser. In the time interval between burning and reading the hole, fluctuations in transition energies can bring molecules into the frequency region of the hole. Therefore, fluctuations in frequency that occur on the time scale from burning to reading the hole will determine the hole width. Since this time scale is typically long (seconds), the experiment will be sensitive to very slow dynamical processes (very slow spectral diffusion). It has been formally proven that hole burning is the frequency-domain equivalent of the stimulated echo experiment.[54,55] The spectrum of the hole is the Fourier transform of the stimulated echo correlation function

$$I_H(\omega_R - \omega_B) \propto \int d\tau \exp[i(\omega_R - \omega_B)\tau] C(\tau, T_w, \tau) \quad (6)$$

where ω_B and ω_R are respectively the burning and reading frequencies. T_w is essentially the time required to do the experiment, from burning through reading.

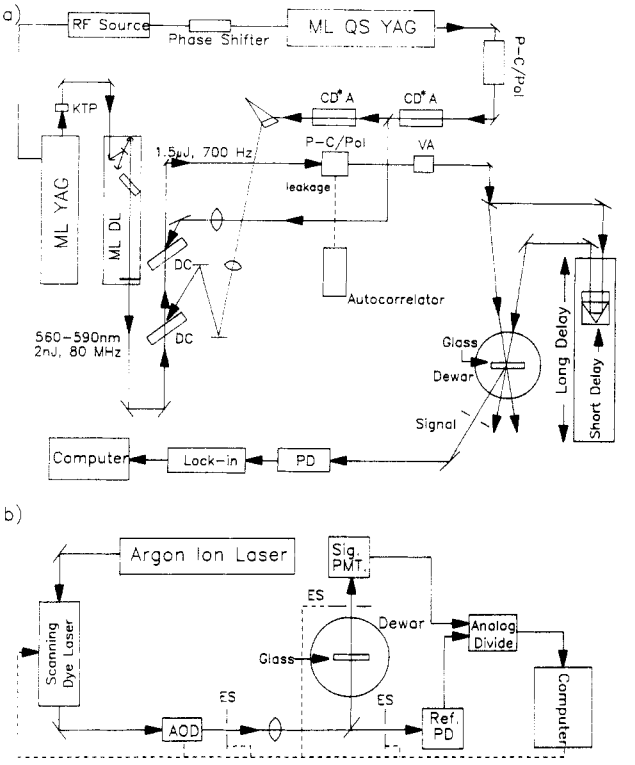

Figure 2. Laser systems used to perform the experiments reported here. (a) Amplified picosecond dye laser system for generation of photon echoes: ML YAG = mode-locked YAG laser, ML QS YAG = mode-locked and Q-switched YAG laser, P-C/Pol = Pockels cell/polarizer pair, DC = flowing dye cell, VA = variable attenuator, PD = photodiode. (b) Narrow-band dye laser system for generation and detection of nonphotochemical holes: AOD = acoustooptic deflector, ES = electrically operated shutter, PMT = photomultiplier tube, PD = photodiode.

The typical time scale for a photon echo experiment is 100 ps. Fluctuations occurring on a microsecond or millisecond time scale are static on the time scale of a photon echo experiment and do not contribute to the measured dephasing time. In contrast, microsecond and millisecond time scale fluctuations are rapid on the seconds time scale of a hole-burning experiment and contribute to the measured dephasing time. Therefore echo and hole-burning experiments should not measure the same dephasing times in systems that have broad distributions of fluctuation rates. Changing the time scale, T_w, of experiments provides a path for the examination of dynamics over a very wide range of times from picoseconds to kiloseconds, or longer.

III. Experimental Procedures

A. Laser Systems

Photon echoes on the organic glasses discussed here used a source capable of producing picosecond pulses of 1–2 μJ at a 700-Hz repetition rate (Figure 2a). The output is attenuated to a few tens of nanojoules for the experiment. The output of an acoustooptically mode-locked Nd:YAG laser is frequency doubled in a KTP ($KTiOPO_4$) crystal and synchronously pumps a dye laser whose output is tunable with a birefringent filter. Pulses are approximately 2 nJ at a repetition rate of 80 MHz. Pulse widths, as measured by an autocorrelator, are 2.4 ps. A separate mode-locked and Q-switched Nd:YAG laser produces a 2-mJ train of approximately 30 pulses at 700 Hz. The largest single pulse is selected

by a Pockels cell and polarizer and is doubled in CD*A (cesium dihydrogen arsenate) to produce a 60-μJ pulse at 532 nm. The leftover infrared is doubled by another CD*A crystal to yield a 10-μJ pulse at 532 nm. Each green beam pumps a stage in a two-stage flowing dye cell amplifier. Dyes used depend on the wavelength of interest and are typically rhodamine 6G or rhodamine B in ethanol or methanol. The two YAG lasers are synchronized by running both mode lockers from the same frequency source. The resulting amplified pulse is separated from the unamplified background by another Pockels cell and polarizer, split with a 30% beam splitter, with one beam sent directly to the sample. The other pulse is sent down a variable-length delay line, a corner cube mounted on a precision optical rail. The two pulses can be separated from 0 to 8 ns with no realignment. The beams are crossed at an angle of 1° in the sample. Noncollinear excitation allows the signal to propagate in a unique direction.[37,56] The signal is detected with a photodiode. A chopper modulates the undelayed beam, and a lock-in amplifier detects the signal at the chopping frequency.

If the sample undergoes hole burning for the laser conditions (power and bandwidth) used in the photon echo experiment, it is of critical importance to correct the echo decays for hole burning. A decay of the echo is recorded at a fixed separation of the pulses (the burning curve). Then a new spot in the sample is selected, and a decay is recorded while the pulse separation is varied by scanning the delay line. Dividing this echo decay by the burning curve gives the true decay as would be observed in the absence of hole burning.[54] This procedure has been thoroughly tested. Echo decays for different intensities and different irradiation times, which result in different extents of hole burning, yield identical dephasing times. The resorufin/ethanol system burns very rapidly while the same dye in ethanol-*d* (deuterated hydroxyl proton) burns negligibly under echo conditions. Echo decays in the former must be corrected for hole-burning effects but the corrections are found to be negligible in the latter. The echo decay times measured in the two systems are identical,[54] indicating that the correction procedure for hole burning is accurate. For materials that do not undergo hole burning for the photon echo laser conditions, e.g., poly(methyl methacrylate) polymers, it is possible to take repeated scans and average the signal, improving the signal-to-noise ratio.

The echo is visible to the eye with approximately 1 μJ in the pair of input beams. This simplifies alignment of the detector. Detailed power-dependent studies are done on each system and the beams are attenuated until the decays are power independent. Typical energies are 20–40 nJ in each beam with a spot size of 200 μm. The laser bandwidth is 10 cm^{-1}. Excitation of higher lying vibrations can add a very fast component to the normal photon echo decay. This is minimized by exciting well to the red of the inhomogeneous absorption maximum. In all cases, echo decay times are independent of excitation wavelength.

Photon echo experiments have been conducted on a wide variety of materials for a quarter of a century. The method is well established and highly reliable. As in any experiment, there can be pitfalls. However, the nature of these is understood and has been carefully checked in these experiments. The echo experiments on chromophores in organic glasses discussed here are completely analogous to those conducted over many years on a wide variety of crystalline and gas-phase systems. Therefore, it is safe to view them as free of artifacts.

Hole-burning experiments are carried out with a frequency-stabilized (2-MHz jitter) scanning dye laser pumped by an argon ion laser (Figure 2b). A hole is burned by exposing the sample to the laser at a fixed wavelength for a given time. After a time interval, the hole is read out by scanning the laser at a much lower power around the burning frequency. The signal is detected in transmission. Electrically operated shutters and modulators are used to control burning times and fluences and to permit the detection of holes as a function of time after burning. Typical fluences are 1–5 $\mu J/cm^2$ for ethanol samples 10–15 $\mu J/cm^2$ for ethanol-*d*. The Völker group has extensively studied the experimental aspects of burning and detecting narrow holes. They find that it is important to use the lowest fluence possible as well as to ensure that only small changes in optical density (hole depth) are induced.[79] In our experiments, holes are less than 2% deep and are in the shallow-hole limit.[79,80] For several samples, e.g., resorufin/ethanol and cresyl violet/ethanol, hole-burning measurements have been carried out by Völker and co-workers. These holes were identical with those measured by the Völker group.[80] The transmitted beam is detected by a cooled photomultiplier, and the input beam is sampled just before entering the Dewar to normalize the signal for laser fluctuations during the scan. A ratiometer divides the signal by the normalization, and the resulting data are stored in a computer for analysis. The samples are excited well to the red of the absorption maximum to avoid contributions from vibrations and to minimize contributions from the phonon sideband. When hole-burning and echo experiments are to be compared, they are performed on the same samples placed in the same liquid helium Dewar. The samples are cooled in the identical manner and the different types of experiments are conducted at the same wavelengths. In both the hole-burning and echo experiments, concentration studies are performed to ensure that the samples are of sufficiently low chromophore concentration that the results are concentration independent.

B. Samples

Most of the experiments reported here have been performed on liquid dye solutions quenched in situ to form glasses. Chromophores studied have included resorufin, cresyl violet, rhodamine B, octadecylrhodamine B, rhodamine 640, and sulforhodamine 640. These molecules are dissolved in a variety of organic liquids such as ethanol, ethanol-*d*, glycerol, and ethylene glycol at typical concentrations of 2×10^{-4} M. Experiments are performed in either an immersion or flow cryostat. The former allows the temperature to be varied between 1.05 and 2.17 K. The latter also permits access to temperatures between 1.5 K and room temperature by controlling the flow of cold helium gas around the sample. Solutions are placed in 1-mm spectroscopic cuvettes and plunged into liquid helium contained in either of the two Dewars, thus forming the

glass. The cooling rate is very high (≫1 K/s), which is essential for ethanol because ethanol can form a partially ordered plastic-crystal phase if cooled too slowly (<1 K/s).[81,82] The photon echo is a "zero background" technique and requires a clear region in the sample on the order of the laser spot size (ca. 200 μm). The quenched liquids are usually full of cracks but sufficient clear regions exist in which the pulses can propagate with a minimum of scatter. It is important to note that in all experiments in which comparisons between echoes and hole burning have been made, the samples have been prepared identically. No special precautions were taken to improve the optical quality of the samples for the echo experiments. Echo and hole-burning experiments were performed on many spots in the same sample. No spot-to-spot differences were observed. The polymer samples used in our studies are made by mixing dye with methylene chloride and poly(methyl methacrylate) powder. A film of the liquid is placed on a microscope slide in a desiccator and the solvent is slowly removed. These samples are solid at room temperature and are of good optical quality. The optical density of all samples is between 0.7 and 1 at the excitation wavelength.

Temperatures below the lambda point of liquid helium are monitored by a Datametrics Barocel pressure gauge. A calibrated four-wire germanium resistance thermometer (GRT) and a precision constant-current source are used for measuring points in the flow cryostat. In this case, the thermometer is mounted close to the point(s) of measurement and the pressure of the gas in the sample chamber is always above 200 Torr. Regulation is good to within ±0.05 K and the temperature measured inside the sample is indistinguishable from that measured on the surface.[83]

IV. Photon Echo Results

Figure 3 displays photon echo decays at 1.5 K from two chromophore-glass systems, resorufin in glycerol glass and cresyl violet in ethanol-*d* glass. The decays are exponential for 5 or more factors of *e*. Using the theory briefly outlined above, one can demonstrate that to observe an exponential decay in a photon echo experiment two conditions must be met. (1) The coupling between the TLS and the chromophores must be via a dipole-dipole interaction.[31,54] (2) The TLS fluctuation rate distribution, $P(R)$, i.e., the probability of the glass having a dynamical process with a rate R, must go as $1/R$ for the rates which have inverses that fall within the experimental time scale.[64] The exponential decays presented in Figure 3 are typical of all systems studied and indicate that the $1/R$ distribution holds for rates from $\approx 1/1$ ps^{-1} to $\approx 1/4$ ns^{-1}.

To derive the two conditions that give rise to exponential decays, the echo correlation function must be averaged over the history of TLS transitions and over the distribution of TLS parameters. Within the TLS model, the modulation of the chromophore's transition frequencies, $\Delta\omega$, arises from sudden jumps between the TLS levels. The correlation function of the echo is written as[55]

$$C(\tau,T_w,\tau) = \exp\{-N(1 - \exp[i\varphi(\tau,T_w)])_{H,r,\lambda}\} \quad (7)$$

H is the average over the history of the jumps, r is over the spatial distribution of the perturbers (TLS), and

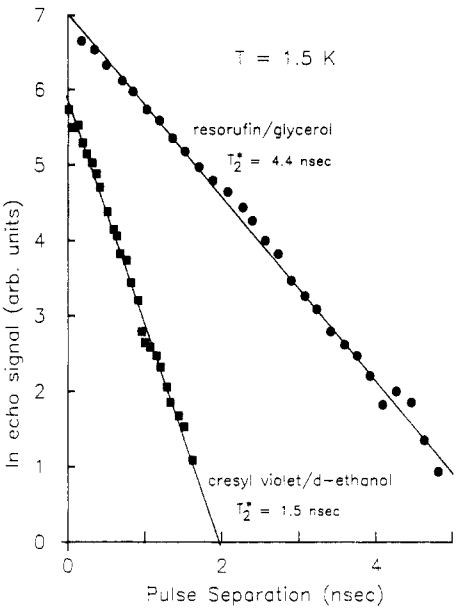

Figure 3. Semilogarithmic plot of photon echo decays in cresyl violet/ethanol-*d* (■) and resorufin/glycerol (●) at 1.5 K. The decays in these and all systems studied to date are exponential. This means that the fluctuation rate distribution $P(R) \propto 1/R$ for rates is from 1/1 ps^{-1} to 1/4 ns^{-1} and that the coupling between the chromophore and the TLS of the glass is dipole-dipole.

λ represents the average over internal TLS parameters. The φ is analogous to the Δ integrals in eqs 3 and 4

$$\varphi(\tau,T_w) = \Delta\omega\left[\int_0^{\tau} h(t)\,dt - \int_{T_w+\tau}^{T_w+2\tau} h(t)\,dt\right] \quad (8)$$

and h is a random telegraph function that can take on values of ±1. The history average has been performed by Hu and Walker using Laplace transform methods for the case of a single rate[84] and recast by Bai and Fayer[55] for a rate distribution as

$$\langle 1 - \exp(i\varphi)\rangle_H = F_1(R\tau,\Delta\omega\tau;x) + F_2(R\tau,\Delta\omega;x)[1 - \exp(-RT_w)] \quad (9)$$

with $x = E/2kT$. For the photon echo experiment, $T_w = 0$, and the second term on the right-hand side of eq 9 vanishes. Therefore, only F_1 needs to be considered to determine the shape of the echo. The F_2 term is of considerable importance in the longer waiting time limit (large T_w) and will be discussed in connection with the hole-burning results. Maynard, Rammal, and Suchail explicitly evaluate F_1 for the case of a $1/R$ distribution of relaxation rates and show that the form of the echo decay is indeed exponential for dipolar TLS-chromophore coupling.[64] The exponential echo decays establish that the fluctuation rate distribution $P(R)$ goes as $1/R$ for dynamical processes occurring on the time scale of the echo experiment.

The distribution of TLS energy splittings and tunneling parameters determines the form of $P(R)$. For $P(R)$ to have the form $1/R$, the distribution of tunneling parameters P_λ must be constant[31,70] (or very close to constant). Therefore the observation of an exponential echo decay immediately provides information on the characteristics of the TLS for the range of tunneling parameters that contribute to the dynamics of the echo time scale at the experimental temperature. It also establishes the coupling mechanism between the TLS and the chromophores.

Figure 4 is a log-log plot of dephasing time versus temperature for three systems, resorufin/ethanol, re-

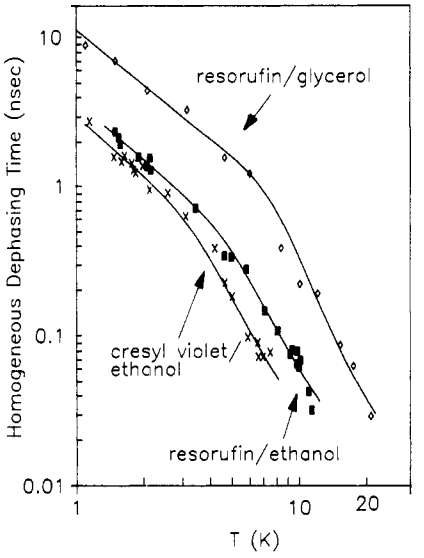

Figure 4. Log–log plots of the temperature dependence of the homogeneous dephasing time, T_2^*, as measured by photon echoes for three systems, cresyl violet/ethanol (×), resorufin/ethanol (■), and resorufin/glycerol (◇). The low-temperature data follow a power law ($T_2^* \propto T^{-\alpha}$, $1.2 < \alpha < 1.6$). This is characteristic of the density of states of TLS at low temperatures. The high-temperature points are influenced by dephasing from an additional activated process (see text).

sorufin/glycerol, and cresyl violet/ethanol. The low-temperature dephasing ($1.3 \leq T \leq 4$ K) follows a power law in which $T_2^* \propto T^{-\alpha}$ with $1.2 \leq \alpha \leq 1.7$. This is characteristic of TLS-induced dephasing and has been observed in many systems by hole-burning experiments.[79,80,82]

Consider the probability, P_E, of having a particular TLS energy splitting E. It is possible to calculate the temperature dependence of the dephasing time as a function of this quantity. If P_E is constant, this dependence will be linear in T.[31,70] It is important to note that a constant distribution of energies (equal probability of having any energy) is the form that leads to a linear term in the theory of the heat capacity of glasses.[29,30] Actual heat capacity measurements yield exponents that are slightly greater than 1, e.g., 1.3.[85] The echo experiments also have exponents, α, greater than 1. The theoretical aspects of the line shape and its variation with temperature have been studied extensively by Small and co-workers,[15] Huber and co-workers,[31,70] and Lyo and Orbach.[77] One common method is to consider P_E which are not constants. To allow some variation in P_E, it is taken to be proportional to E^μ, where μ is a small constant.[41] Berg et al. showed that T_2^* is

$$T_2^* = A(kT)^{-(1+\mu)} \tag{10}$$

where A is a collection of constants.[54] Setting $0.2 \leq \mu \leq 0.7$ accounts for the experimental results. Specific heat measurements on silicate glasses have also shown that P_E is proportional to $E^{0.3}$, which is consistent with the values obtained from optical dephasing experiments on organic glasses.[40]

At higher temperatures, the data deviate markedly from the power law and are better described by an activated process. This can be clearly seen by examining the resorufin/glycerol system (where the slow TLS dephasing allows the temperature study to be extended to 20 K) on an Arrhenius plot (Figure 5). Exponentially activated dephasing has been observed in mixed molecular crystals.[71,86,89] Jackson and Silbey have argued that this type of behavior should also be present in glasses,[87,88] and all of the glass photon echo data can be well fit by a form

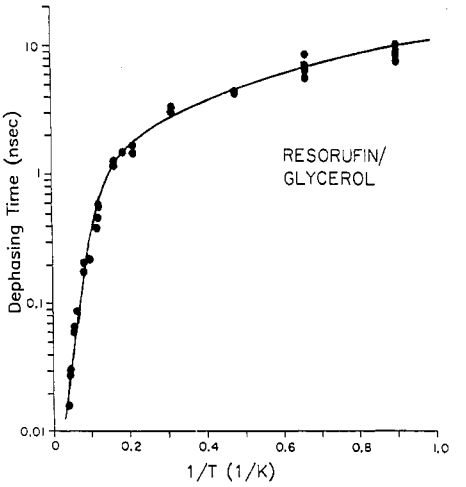

Figure 5. Arrhenius plot of the homogeneous dephasing time in the resorufin/glycerol system. The slow dephasing characteristic of this glass enables study of dephasing to 20 K. The high-temperature points fall on a straight line, indicating an activated process.

$$1/T_2^* = aT^\alpha + b(T)e^{-\Delta E/kt} \tag{11}$$

In crystals, the activated process is due to localized motions of the chromophore in the host lattice.[71,86,89] Recent experiments indicate, however, that the mechanism may be fundamentally different in glasses in that an optical phonon of the host glass as opposed to a localized motion of the guest is responsible for the high-temperature dephasing.[66] Figure 6a shows the result of a photon echo study of rhodamine B and octadecylrhodamine B in a PMMA host. The two molecules are identical except that the latter has an 18-carbon chain attached to it in place of the acid proton of the former. The masses and moments of inertia of these molecules are vastly different. This means that any localized translational or rotational motions of the molecules will be different and give rise to different activation energies, ΔE. The temperature-dependent dephasing data, however, are identical over all temperatures studied. Figure 6b shows that decays taken at the same temperature from each sample are superimposable. This demonstrates that the high-T dephasing, at least in PMMA, cannot be a property of the chromophore but must be caused by some mode of the glass. If acoustic phonons are responsible, one would expect that the high-temperature points would have a T^{-7} temperature dependence as observed in ruby.[16,21,72] In all experiments to date, however, a single activation energy fits all of the high-temperature points well, suggesting that the mode must have a very narrow distribution of energies and is therefore more characteristic of an optical phonon. Because of the disorder in the glass, the optical phonon responsible for the dephasing may be localized.

V. Hole-Burning Results

Figure 7 shows holes burned in cresyl violet, resorufin, and sulforhodamine 640 in ethanol glasses as well as the

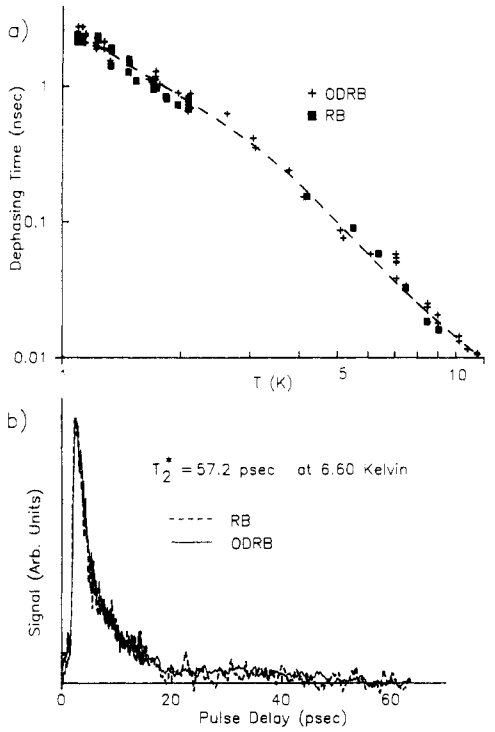

Figure 6. Nature of high-temperature dephasing. (a) Log–log plot of the homogeneous dephasing time in rhodamine B (RB) and octadecylrhodamine B (ODRB) in poly(methyl methacrylate) (PMMA). Although the two chromophores have very different masses and moments of inertia, the temperature dependences are identical. (b) Comparison of two echo decays, RB/PMMA and ODRB/PMMA, at 6.60 K. The decays are superimposable. Taken together with the data of (a), this means that the mode responsible for dephasing at high T in PMMA is a property of the polymer matrix and not some localized motion of the chromophore as is the case in crystalline systems.

analogous line width obtained by taking the Fourier transform of the photon echo measurements on the same substances at the same temperature. The measured hole widths agree with those reported by other laboratories.[80] In each case, the hole line width is significantly broader than the echo line width. This confirms the contributions of spectral diffusion to the measurement. The hole width is dominated by slow time scale energy evolution of the system (spectral diffusion) while the photon echo line width only has contributions from fast fluctuations (homogeneous broadening).

It is important to distinguish between the hole-burning mechanism and the hole-broadening mechanism. The echo decays for cresyl violet and sulforhodamine 640 were obtained in ethanol-*d*. The deuterated hydroxyl group reduces the hole-burning efficiency by approximately a factor of 60[54,90] and greatly simplifies collection of the echo data. This implies that hydrogen bond rearrangements are involved in the hole-burning mechanism. Figure 8 shows a study of the hole-burning efficiency of resorufin in ethanol/ethanol-*d* mixtures. The dependence is quadratic with the mole fraction of ethanol, demonstrating that a double hydrogen bond rearrangement is the structural change responsible for hole burning. However, the hole widths and echo decays are *not* affected by deuteration, which means that optical dephasing and hole burning involve different mechanical degrees of freedom in the glass.

Figure 9 shows temperature-dependent hole-burning data on the cresyl violet and resorufin in ethanol systems. Once again, the low-temperature data can be fit well to a power law of the type $T^{\sim(1.2-1.6)}$. This behavior has been observed by many groups.[79,80,82] The high-temperature points have additional dephasing from an exponentially activated process just as in the echo experiments. The effect is much less noticeable than in the echo experiments because a large amount of TLS broadening from spectral diffusion masks the influence of the activated process. The hole shapes are Lorentzian, the Fourier transform of an exponential decay. This demonstrates that the coupling between the chromophore and TLS is dipole–dipole,[31,70] which is consistent with the exponential echo decays. The coupling mechanism between the chromophore and the TLS is the same for fast and slow fluctuations.

The difference between the two techniques suggests that hole-burning experiments will show changing widths as a function of time between burning and

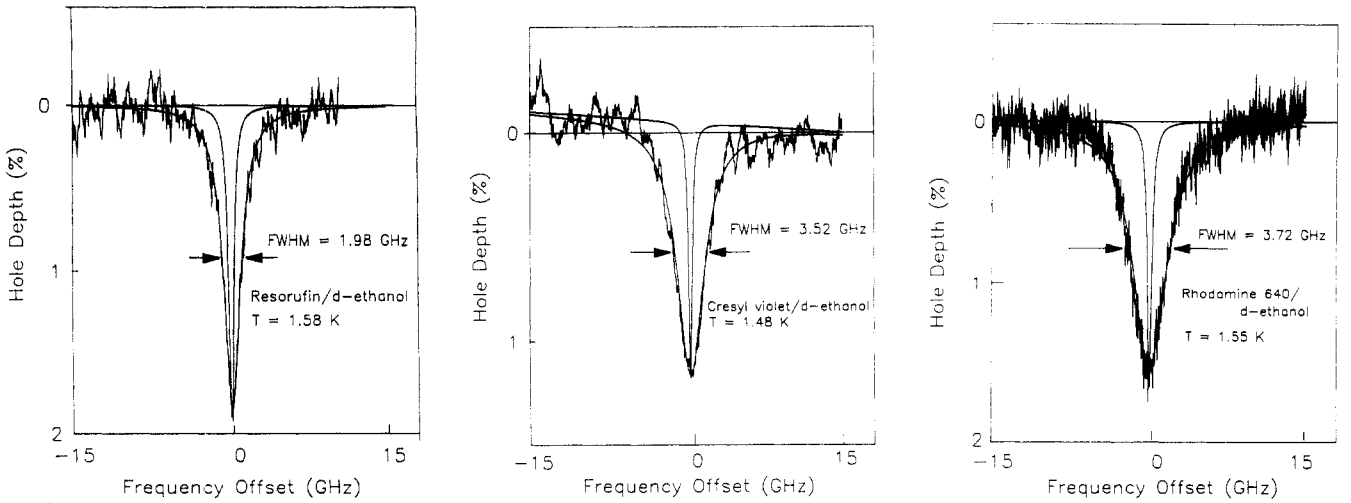

Figure 7. Comparison of hole line widths burned in resorufin/ethanol-*d*, cresyl violet/ethanol-*d*, and sulforhodamine 640/ethanol-*d* with the corresponding line widths obtained from the Fourier transform of photon echo data on the same systems at the same temperature. The holes are Lorentzian, which means that the chromophore–TLS coupling is dipole–dipole. All of the line widths obtained from the photon echo data are significantly narrower than the measured hole widths, meaning that the hole-burning experiment is affected by slow spectral diffusion caused by structural relaxations of the glass occurring in the approximately 100 s required to burn and read a hole (T_w).

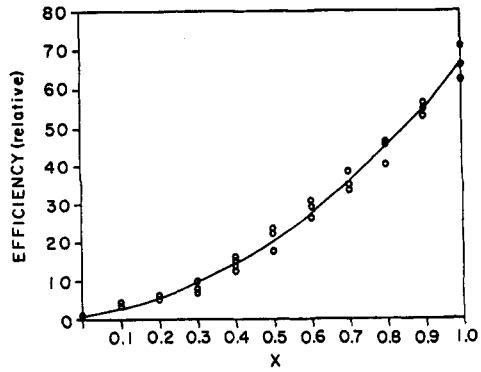

Figure 8. Relative hole-burning efficiency of resorufin in ethanol/ethanol-*d* mixtures. x is the mole fraction of ethanol-*d*. The quadratic concentration dependence indicates that a double hydrogen bond rearrangement is responsible for hole burning. Although the hole-burning efficiency is drastically affected by deuteration of the hydroxyl proton, the measured hole widths and echo decays are identical. Thus the hole-burning mechanism and optical dephasing involve different modes of the glass.

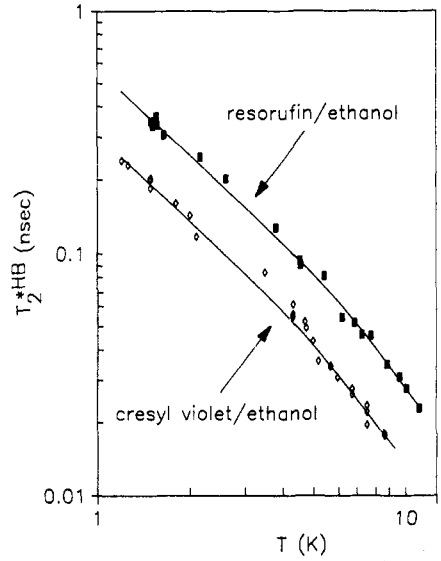

Figure 9. Log–log plots of the temperature-dependent dephasing times in cresyl violet/ethanol (◇) and resorufin/ethanol (■) as measured by hole burning. The times are much shorter than those measured by photon echoes on the same systems (Figure 4). The low-temperature points follow the power law characteristic of TLS dephasing, and the high-temperature points are affected by an exponentially activated process just as in the photon echo data. The activated process at high temperature is partially masked by the broadening of the hole by the extensive spectral diffusion occurring between burning and readout.

reading. As discussed in the Introduction, this has been extensively studied by Shelby and Macfarlane in the spin-active Pr^{3+}:CaF_2 crystal[48] and in the long-time hole-burning measurements of the Haarer group,[20,50] who burned photochemical holes in quinizarin/ethanol–methanol mixtures and read them over a period of several days. The hole widths increased slowly on a logarithmic time scale for quinizarin/(3:1 EtOH:MeOH). They concluded that most of the broadening occurred within the first 10 min of the experiment. In a time-dependent hole-burning experiment, changing the reading time after burning amounts to scanning the T_w. Hole burning is the Fourier transform of the stimulated echo. Using the formalism discussed above, Bai and Fayer[55] showed that these measurements are an experimental route to deducing the form of $P(R)$ without assuming a specific model of glass dynamics.

As discussed earlier, the hole burning observable is T_w dependent, and the spectral diffusion contribution to the line width depends on the second term in eq 9

$$F_2(R\tau,\Delta\omega\tau;x)\{1 - \exp(-RT_w)\} \quad (12)$$

In the limit that $R,1/T_w \ll 1/\tau$, the case for all hole-burning experiments conducted to date, $F_2 = \sin^2(\Delta\omega\tau)\,\mathrm{sech}^2(x)$ and is independent of T_w. When combined with the T_w-dependent exponential term, the function is constant over the interval $1/\tau > R > 1/T_w$ and falls sharply to zero elsewhere. This is a "window" which depends on T_w, and it selects for observation those processes that are active on the time scale between τ and T_w.[49,55] In the long waiting time limit ($T_w \gg 10\tau$), in which all hole-burning experiments have been performed, the correlation function is[55]

$$C(\tau,T_w,\tau) = \exp\{-N\langle \sin^2(\Delta\omega\tau)\,\mathrm{sech}^2(E/2kT) \times \{1 - \exp(-RT_w)\}\rangle_{r,\lambda}\} \quad (13)$$

The averages over r (TLS spatial distribution) and R can be performed. The resulting dependence of the hole width on waiting time is

$$\Delta\nu_H \propto -\int dR\, P(R)[1 - \exp(-RT_w)] + \text{contributions from } T_w \text{ independent fast fluctuations} \quad (14)$$

Determining $P(R)$ involves measuring hole width vs T_w and comparing the data to eq 14 using a model of $P(R)$. The contribution to the hole width that is T_w independent can be obtained from the echo data. The rate distribution, however, is determined by the way the hole width changes with T_w on the long time scale and can be obtained even in the absence of echo data. Such an experiment has recently been done by Littau et al. on cresyl violet in ethanol, ethanol-*d*, and glycerol glasses.[68] Figure 10a shows three holes measured at different times after burning in the cresyl violet/ethanol system. As the time between burning and reading increases, the hole broadens.

Figure 10b shows the results of a complete waiting time dependent hole width study for cresyl violet in ethanol at 1.30 K. The hole width is seen to vary over the entire range of study, but the change in width (on a logarithmic time scale) is most pronounced in the range of 50 s. Even without the theoretical development presented briefly above, one could conclude that there exists some process with a characteristic rate around $1/50\ s^{-1}$ in this system. This qualitative information allows one to select a trial form of the fluctuation rate distribution function, $P(R)$. Since convolution with the function $1 - \exp(-RT_w)$ according to eq 14 tends to smooth out any sharp features, there is little point in selecting an excessively complicated form for the fluctuation rate distribution function. A log normal distribution (Gaussian on a logarithmic time scale) was found to be the simplest form that fit the data well. Note that this is by no means a unique solution to the problem of finding $P(R)$. Other functions will also fit the data, for example, a rectangular distribution. However, all functions that fit the data have three features in common—identical center frequencies, identical areas under the curve, and the same characteristic widths. A function that does not contain all of these properties, i.e., a delta function, will not fit the

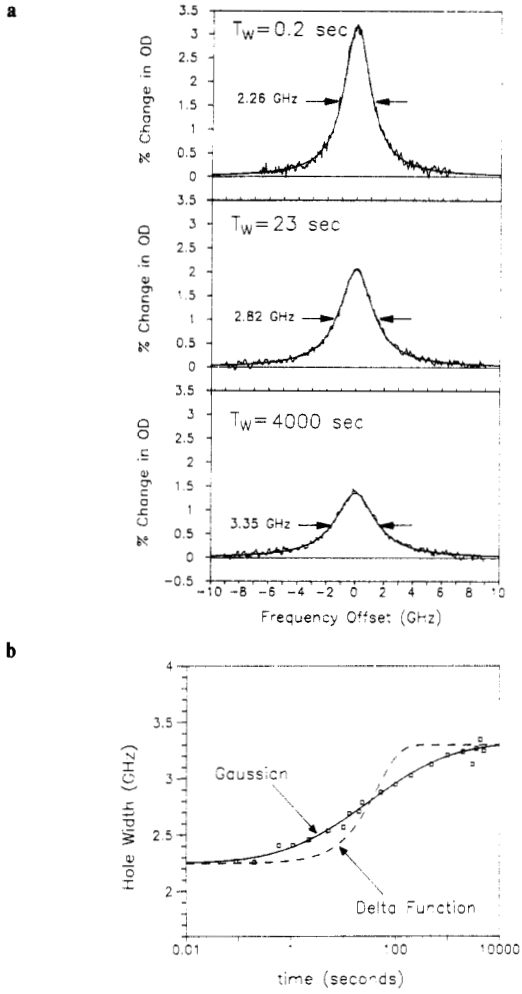

Figure 10. Time-dependent hole-burning results. (a) Holes burned in cresyl violet/ethanol detected as a function of time after burning (scanning T_w). The hole widths increase substantially with time. This directly confirms the prediction of time-dependent hole widths suggested by comparison of photon echo and hole-burning data. (b) Semilogarithmic plot of hole width as a function of time in cresyl violet/ethanol at 1.3 K. The lines are obtained by evaluating eq 14 with rate distributions $P(R)$. The dashed line is for $P(R)$, a delta function (only one rate), and does not fit the data. A log normal distribution ($P(R)$ is a Gaussian on a logarithmic scale) matches the data extremely well. The distribution is centered around a rate $R_0 = 0.02\ s^{-1}$ with a variance $\sigma = 3.8$.

data. A log normal distribution exhibits all properties and is the most physically reasonable. In addition, it fits the data slightly better than unphysical functions such as rectangular distributions. Therefore it will be used in the analysis of the data. If the dephasing is due to TLS and the relaxation of the TLS is caused by phonon-assisted tunneling, then a log normal distribution of fluctuation rates is equivalent to a Gaussian distribution of tunneling parameters.[43,68] Such a distribution of tunneling parameters has been used in the analysis of thermodynamic properties, such as time-dependent heat capacities of amorphous silica[91] and the kinetics of the hole growth process.[42,43]

Explicitly the best fit to the data was achieved when

$$P(R)\ dR \propto \exp[-(\ln (R/R_0))^2/\sigma^2]\ d(\ln R) \quad (15)$$

where $\ln (R_0 \times 1\ s) = -3.9 \pm 1.0$ and $\sigma = 3.8 \pm 1.0$. The errors listed are obtained by defining $\chi^2 = \sum_i([y_i - f(i)]/\mathrm{ERR}_i)^2)$ and including in the limits all fits where $\chi^2 \leq$ (no. of data points − no. of free parameters). The solid line in Figure 10b is a plot of the best fit using this

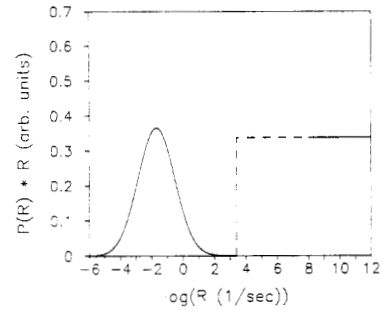

Figure 11. The fluctuation rate distribution in ethanol glass at 1.3 K based on photon echoes and time-dependent hole burning. The horizontal line on this semilogarithmic plot (short times, fast rates) indicates that $P(R) \propto 1/R$ and is obtained from the exponential photon echo decays. The Gaussian at long times (slow rates) is a result of the time-dependent hole-burning measurements. The intermediate-time regime (dashed line) is currently under investigation.

function. The dashed line in Figure 10b is an example of the best fit possible when the form of $P(R)$ is assumed to be a delta function; i.e., there is a single rate rather than a broad distribution of rates. One can see that it cannot be made to fit the data nearly as well as the log normal distribution, indicating the underlying fluctuation rate distribution does have an intrinsic width. Indeed, two delta functions still fail to adequately reproduce the data. When the number is raised to three with freely floating individual rates, the fit becomes better but is still not as good as the log normal distribution, and there are too many free parameters to achieve a unique fit. The experiment was repeated at 2.13 K. A log normal distribution was again used to fit the data at the higher temperature. The best fit was obtained when $\ln (R_0 \times 1\ s) = -3.7 \pm 1.0$ and $\sigma = 3.8 \pm 1.0$. Note that $P(R)$ changes very little with temperature. The center of the distribution remains close to $1/50\ s^{-1}$. This is consistent with the TLS theory in which the relaxation rate is weakly dependent on temperature.[29,30] Descriptions of glass dynamics other than tunneling TLS tend to predict much more dramatic temperature dependences (see below).

Figure 11 is a plot of the fluctuation rate distribution used to fit the 1.3 K data in Figure 10b. It is produced from a combination of these hole-burning results and the photon echo data taken on the same sample.[65,68] The hole-burning results, in addition to yielding eq 15, give the area under the fluctuation rate distribution curve for rates faster than the inverse of 10 ms.[68] From the echo data, one may calculate the form of $P(R)$ out to the coherence time of the sample (here 10 ns).[65] As discussed above, $P(R) \propto 1/R$ in this region.[65] The $1/R$ distribution when plotted as $P(R) \times R$ is a horizontal line. Note that the form of $P(R)$ between 10 ns and 10 ms is unknown. Only the total area under the $P(R)$ curve is known. The dashed line in Figure 11 is the result that would occur assuming the $1/R$ distribution continues past 10 ns unchanged until forced to cut off by the area constraint. In light of the slow rate results presented here, it is likely that the distribution is more structured than is indicated by the dashed line in Figure 11. Waiting time dependent experiments performed in this region will clarify the nature of the rate distribution. These time-dependent results are the first to record and analyze the dynamic modes of a glass on this time scale.

However, while the results described above quantitatively define the dynamics, they still leave open the question of what is the source of these modes. To check this, the same type of experiment was carried out on the system resorufin in ethanol at 2.13 K. The data show that the hole width again broadens in a manner similar to cresyl violet in ethanol—most quickly in the range of $1/50$ s^{-1}. Fitting the distribution using the form of $P(R)$ in eq 15 yields the parameters ln (R_0 × 1 s) = -2.9 ± 0.8 and $\sigma = 4.2 \pm 0.8$. These values are within experimental error of the parameters obtained for the system cresyl violet in ethanol at 2.13 K. In terms of its physical properties, resorufin is dramatically different from cresyl violet. Resorufin's net negative charge should influence its surroundings in a drastically different manner than positively charged cresyl violet. If these dye molecules are themselves the TLS responsible for glass dynamics, there is little chance that they would yield the identical fluctuation rate distribution. The fact that the experiments yield the same form for $P(R)$, for the ranges of R's studied, indicates that the dynamic modes on this time scale are intrinsic to the ethanol glass and are not strongly influenced by the presence of the dye molecule. The $P(R)$ distributions for the two dyes differ in the absolute amount of broadening. This is of no concern, however, since the broadening is directly proportional to the TLS–chromophore coupling strength, which is dependent on the choice of dye regardless of the nature of the TLS. In fact, the ratio of the absolute amount of broadening in the two systems is equal to the ratio of the coupling strengths assuming the choice of dye does not severely influence the nature of the glass TLS.[55] The ratio of the amount of broadening from 0.01 to 5000 s in the case of cresyl violet/resorufin in ethanol is 1.7. This is in good agreement with the ratio of the photon echo line widths of the two systems, which is also equal to the ratio of the coupling strengths – cresyl violet/resorufin two-pulse echo line width = 1.6. This indicates that the coupling strength is basically independent of relaxation rate. While not conclusive, this result is highly suggestive that the coupling mechanism is identical at both short and long times.

Since the dynamics proved to be independent of dye molecule, an experiment was performed on an entirely different glass, resorufin in glycerol. Extensive hole-burning and photon echo results have been reported for this system.[55,92,93] The difference between the line widths obtained by hole burning and two-pulse photon echoes is only a factor of 3 for this system as opposed to a factor of 8 for cresyl violet in ethanol.[55,65,92] This implies that there is substantially less dynamic activity between the time scales of the two-pulse echo and hole burning in the glycerol system. One might expect, therefore, to see little in the way of hole broadening. This is exactly the case. There is essentially no change in hole width over 3 orders of magnitude in time—from 5 s out to 4000 s.[92] There is only the slight suggestion of a change at very fast times, 0.1–0.5 s. The change is too small to make any predictions about the $P(R)$ distribution at the faster times. However, this result serves as a good counterexample to the results obtained in ethanol, where a dramatic change was seen, and serves as a further confirmation of the validity of the ethanol measurements. Any phenomena not intrinsic to the glass itself which might be suggested as a source of the observed time-dependent hole broadening, i.e., systematic errors, should have been observed in the glycerol system just as in the ethanol system. The absolute magnitude of the hole width in glycerol is different from that reported in previous studies.[93] However, it has been shown that the hole width of resorufin in glycerol is highly dependent upon cooling rate, slower cooling rates yielding narrower hole widths.[92] The glycerol sample in this experiment was quickly cooled as detailed in section III. The hole widths recorded in this experiment agree with those taken on a similarly prepared sample using time-independent hole-burning techniques.[55,92]

VI. Temperature-Cycled Hole-Burning Experiments: A Detailed Test of the TLS Model

As mentioned in the Introduction, the TLS model is not the only one offered to account for the unusual properties of low-temperature glasses. Most of the other ideas are based on the dynamics of defect states.[32,95] The essential difference is that the TLS model postulates the existence of fixed potential surfaces modeled as a distribution of double wells while in the other models, the surfaces evolve in time.[32] A critical test of the fixed-potential hypothesis is a temperature-cycled hole-burning experiment in which a hole is burned and read at a low temperature, taken to a higher temperature, read, returned to the lower temperature, and again read. If the TLS model holds, the hole will broaden at the higher temperature and the broadening will be completely reversible when the system is returned to the lower temperature. In order to test the TLS model, both temperatures of the temperature cycle must be in the range of temperatures where quantum tunneling is the dominant dephasing mechanism.

If, on the other hand, at the high temperature, thermal hopping begins to appear as the dominant TLS transition mechanism, this would yield an exponential (or multiexponential) dependence on temperature and an irreversible hole width. Irreversible temperature-cycling hole widths have been reported for many systems by Friedrich, Haarer, and co-workers.[20,50,95] However, with the exception of a very few cases,[95] waiting time dependences have not been measured, and in no previous study has the waiting time dependence been determined at both the low and high temperature. In the cresyl violet/ethanol system, one would surmise that the hole width is not completely reversible if one did not take the T_w dependence into account. In addition, there is little irreversibility reported in the systems studied previously until the samples are cycled to temperatures of 5–10 K.[20,50,95] These temperatures, as the authors suggest, are in the range where the tunneling mode of the TLS dynamics begins to break down in favor of a thermal hopping mechanism. When the entire experiment is done in the range where tunneling TLS dominate and when the T_w dependence is accounted for, the hole width should be reversible if the TLS model holds, as is documented below.

The results of the temperature-cycling experiment[96] are detailed in Figure 12. The solid lines are the time dependences of the hole width at 1.30 and 2.13 K. The dashed line is a predicted response calculated with no

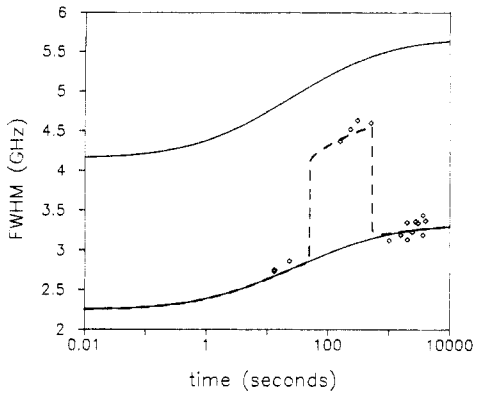

Figure 12. Results of a temperature-cycled hole-burning experiment on cresyl violet/ethanol. A hole burned at 1.3 K and cycled to 2.1 K assumes its long waiting time width after being returned to 1.3 K. The dashed line is a calculation without adjustable parameters using eq 24, which describes the experiment. The agreement shows that the fixed-potential assumption of the TLS model is valid and that other models, e.g., defect or particle diffusion, are not valid descriptions of glass behavior.

adjustable parameters using the data taken at 1.30 and 2.13 K. The details of the calculation are shown below. The key feature is that, after returning to the original temperature, the hole width returns to the value expected without a temperature cycle. That is, the temperature-dependent line broadening is totally reversible. This result indicates that the glass returns to the same configurational minimum after a temperature cycle as it occupied before the temperature was raised.

A theoretical analysis will be presented demonstrating the remarkable agreement between the results of the temperature-cycling experiment and the TLS model of glass dynamics. First, however, the problem may be described more qualitatively. Assume the hole is burned at a temperature T_0. According to the TLS model, the TLS with $E \leq kT_0$ are constantly fluctuating and, therefore, contribute to hole broadening. The TLS with $E > kT_0$ are frozen in their ground states. Thus, the width of the hole shortly after burning is only determined by the low-energy TLS. When the temperature is raised to T_1, additional TLS with $kT_0 \leq E \leq kT_1$ become active and contribute to hole broadening. When the temperature is returned to T_0, these higher energy TLS return to their ground states. The chromophores that make up the hole experience a configuration associated with the higher energy TLS identical with that experienced when the hole was burned. Thus, the hole width is again determined only by TLS with $E \leq kT_0$, and the sample retains no knowledge that it ever was cycled to a higher temperature. This model is presented in contrast to a particle or defect diffusion model where the structure of the glass is continually evolving in time. In a diffusion model (analyzed in the Appendix), raising the temperature would increase the rate of the diffusive motion. When the temperature was again lowered, the diffusive motion would slow again but continue to randomize the local structure, showing no reversible behavior.

An equally accurate description of the fixed potential surface model focuses on the motion of the glass configuration upon its potential energy surface. When the temperature is low, $T = T_0$, the glass configuration may wander upon its N-dimensional potential surface, limited only by the restrictions that it cannot access states where $E > kT_0$ or where the transition rate to that state is vanishingly small. This range of motion on the potential surface corresponds to the width of the hole detected at T_0. When the temperature is raised to T_1, the glass may now access different states, i.e., those states where $kT_0 < E < kT_1$. This leads directly to a broader hole at T_1. When the temperature is lowered again, the glass structure returns to those states where $E < kT_0$, and the hole width narrows accordingly. Here it may be seen why it is necessary that the relaxation rate be weakly (linearly or sublinearly) related to temperature. If, at the high temperature, the glass configuration accesses states (by thermal hopping) that have vanishingly small relaxation rates at T_0, the glass would be frozen in the high-temperature configuration, and the hole width would not narrow again on the time scale of the experiment. This requirement of weak temperature dependence is satisfied in the TLS model, where quantum tunneling is the dominant transition mechanism.

The temperature-cycling experiment will now be analyzed quantitatively in terms of the TLS model, and the diffusion model is analyzed in the Appendix. The TLS model has been successful in describing the results of photon echo and hole-burning measurements in glasses.[1,19,29,30] The observed Lorentzian hole shapes and the quasilinear temperature dependence of the hole widths can be derived within the TLS framework.[97,98] However, it is possible to explain previous optical experiments with a defect or particle diffusion model, as has been done for heat capacities[32,99] and other experiments on glasses. The reversibility of the temperature-cycled hole widths is a property that cannot be explained with a model based on diffusion. An argument in support of this point based upon the correlation function for a diffusing system is made in the Appendix. In the following discussion, the TLS model is used to predict the results of a temperature-cycling study, and the predicted results are compared to the experiment. The analysis of the temperature-cycling hole burning using the TLS model is identical with that of standard hole burning except in the calculation of the history average. It was implicitly assumed above that burning and reading were at the same temperature. When this is not the case, the probability that the TLS has changed state in the time between burning and reading is modified. The form of the history average is

$$\langle 1 - \exp(i\varphi)\rangle_H = p_{+-}\{1 - \exp(2i\Delta\omega\tau)\} + p_{-+}\{1 - \exp(-2i\Delta\omega\tau)\} = \operatorname{sech}^2(E/2kT)\sin^2(\Delta\omega\tau)[1 - \exp(-RT_w)] \quad (16)$$

The joint probability of finding the TLS in the upper (lower) energy state at $t = 0$ and in the lower (upper) energy state at $t = T_w$ is

$$p_{+-} = \rho_+(0)\rho_-[T_w|\rho_+(0) = 1]$$
$$p_{-+} = \rho_-(0)\rho_+[T_w|\rho_-(0) = 1] \quad (17)$$

where ρ_+ (ρ_-) is the upper (lower) population density of the TLS with respect to its local field. $\rho_-[T_w|\rho_+(0) = 1]$ is the conditional probability of the TLS being in the lower state at T_w assuming the TLS was in the upper state at $t = 0$. $\rho_+[T_w|\rho_-(0) = 1]$ is defined similarly. Substituting eq 17 into eq 16, one obtains the general result of the history average

$$\{\rho_+(0)\rho_-[T_w|\rho_+(0) = 1] + \rho_-(0)\rho_+[T_w|\rho_-(0) = 1]\} \sin^2(\Delta\omega\tau) \quad (18)$$

Here we have taken into account that the sign of the coupling $\Delta\omega$ is uncorrelated to the orientation of the local field experienced by the TLS. Therefore, the imaginary parts in eq 16 cancel. When the spatial average yields a Lorentzian hole (exponential decay of the correlation function), as has been usually observed, it is straightforward to show that the width of the hole is given by[68]

$$\Delta\omega_H(T_w) \propto \langle\{\rho_+(0)\rho_-[T_w|\rho_+(0) = 1] + \rho_-(0)\rho_+[T_w|\rho_-(0) = 1]\}\rangle_\lambda \quad (19)$$

Thus the entire problem reduces to solving the equation of motion of the TLS. Take the temperature cycle to be described by a step function, i.e.

$$T(t) = T_0 \qquad t \le t_1 \quad (20a)$$

$$T(t) = T_1 \qquad t_1 \le t \le t_2 \quad (20b)$$

$$T(t) = T_0 \qquad t > t_2 \quad (20c)$$

The initial population distributions are $\rho_+(0) = \rho_+(eq;T_0)$ and $\rho_-(0) = \rho_-(eq;T_0)$. The conditional probability $\rho_-[T_w|\rho_+(0) = 1]$ for the TLS may then be calculated. To find $\rho_-[T_w|\rho_+(0) = 1]$ it is necessary to derive an expression for $\rho_-(T_w)$ for any initial condition. This can be shown to be[68]

$$\Delta\rho(t) - \Delta\rho(eq) = [\Delta\rho(t_0) - \Delta\rho(eq)] \exp(-R(t - t_0)) \quad (21)$$

This can be solved for $\rho_-(t)$. The solution is

$$\rho_-(t) = (1/2)[1 - \Delta\rho(eq) + (\Delta\rho(eq) - \Delta\rho(t_0)) \times \exp(-R(t - t_0))] = \rho_-(eq) + (\rho_-(t_0) - \rho_-(eq)) \exp(-R(t - t_0)) \quad (22)$$

At this point, the temperature-cycling conditions are inserted. During the first interval, $T_w \le t_1$, the conditions are exactly the same as in the fixed-temperature experiment. During the second and third time intervals, the conditional probabilities are found by letting $t_0 = t_1$ and $t_0 = t_2$, respectively. This gives

$$\rho_-[T_w|\rho_+(0) = 1] = \rho_-(eq;T_0)\{1 - \exp[-R(T_0)T_w]\} \qquad T_w \le t_1 \quad (23a)$$

$$\rho_-[T_w|\rho_+(0) = 1] = \rho_-(eq;T_1)\{1 - \exp[-R(T_1)(T_w - t_1)]\} + \rho_-(t_1) \exp[-R(T_1)(T_w - t_1)] \qquad t_1 \le T_w \le t_2 \quad (23b)$$

$$\rho_-[T_w|\rho_+(0) = 1] = \rho_-(eq;T_0)\{1 - \exp[-R(T_0) \times (T_w - t_2)]\} + \rho_-(t_2) \exp[-R(T_0)(T_w - t_2)] \qquad T_w > t_2 \quad (23c)$$

One can show that $\rho_+[T_w|\rho_-(0) = 1]$ has the same form.

For single-phonon-assisted resonant tunneling, the relaxation rate is very weakly dependent on the temperature, $R(T) \approx \coth(E/2kT)$.[29,30] Because $R(T)$ is, at most, linear in temperature, the relaxation rates change by much less than a factor of 2 in the temperature range of interest, i.e., 1.3–2.1 K. Taking the exact temperature dependence of R into account greatly complicates the problem. Since spectral diffusion takes place on a logarithmic time scale, the difference between the predictions of the cycled hole width using the exact form of $R(T)$ and considering $R(T)$ to be constant is imperceptible. That is, the difference is well within the signal to noise in this experiment. Therefore, in the temperature range of interest, it can be taken to be independent of T, $R(T_1) = R(T_0)$. This is consistent with experimental observations (see discussion given above of the log normal rate distributions at the two temperatures). Thus, it is easy to see that eq 23c becomes identical with eq 23a in the long waiting time limit, $T_w \gg t_2$. In practice, this condition can always be satisfied in a waiting time dependent hole-burning measurement because spectral diffusion broadens the hole on a logarithmic time scale. Since eq 23a describes the situation where no temperature cycling is present, this indicates that the temperature cycle does not affect the long-time behavior of the hole spectrum. To calculate the temperature-cycling data, it is necessary to average over all of the TLS. We reduce the average over the internal parameters of the TLS in eq 19 to an average over the fluctuation rate distribution. The details of this conversion are given in ref 68. The final expression for the time evolution of the hole width including the temperature cycle is

$$\Delta\omega_H(T_w) = \Delta\omega_0\langle 1 - \exp(-RT_w)\rangle_R \qquad T_w \le t_1 \quad (24a)$$

$$\Delta\omega_H(T_w) = A\Delta\omega_0\langle 1 - \exp[-R(T_w - t_1)]\rangle_R + \Delta\omega_0\langle\exp[-R(T_w - t_1)] - \exp(-RT_w)\rangle_R \qquad t_1 \le T_w \le t_2 \quad (24b)$$

$$\Delta\omega_H(T_w) = \Delta\omega_0\langle 1 - \exp[-R(T_w - t_2)] + \exp[-R(T_w - t_1)] - \exp(-RT_w)\rangle_R + A\Delta\omega_0\langle\exp[-R(T_w - t_2)] - \exp[-R(T_w - t_1)]\rangle_R \qquad T_w > t_2 \quad (24c)$$

where A is a scaling constant given by the ratio

$$\langle\rho_+(eq;T_0)\rho_-(eq;T_1) + \rho_-(eq;T_0)\rho_+(eq;T_1)\rangle_E/2\langle\rho_+(eq;T_0)\rho_-(eq;T_0)\rangle_E \quad (25)$$

Here we have taken R to be independent of temperature. The relative population densities at equilibrium in eq 25 are related to temperature according to $\rho_\pm(eq;T) = (1 + \exp(\pm\beta E))^{-1}$, where $\beta = 1/kT$. The averages over E in eq 25 must be done using the appropriate density of states. It has been shown that, using the TLS model, the density of states of TLS may be related to the temperature dependence of the hole width in a simple fashion.[54] $P(E) \propto E^{\alpha-1}$, where α is the exponent of the temperature in the temperature dependence; i.e., $\Delta\omega_H(T) \propto T^\alpha$. By examining the data in Figure 12, one can calculate the density of states for the TLS in ethanol. For rates faster than 100 s^{-1}, $P(E) \propto E^{0.2}$. This is consistent with the results of the temperature dependence of the echo decay rate, $T^{1.3\pm0.1}$.[65] For rates slower than 100 s^{-1}, $P(E) \propto E^{0.3}$. This is the regime where the fluctuation rate distribution $P(R)$ is described by a log normal function.

In Figure 12, eq 24 is plotted without adjustable parameters (dashed line) using the information obtained from fitting the standard waiting time dependent hole-burning measurements (no temperature cycle) at 1.30 and 2.13 K. The temperature-cycling times are t_1 = 50 s and t_2 = 500 s. The agreement between experiment and the theory based on the TLS model is quite remarkable.

It has been assumed for many years, without conclusive evidence, that the TLS model is an accurate description of of low-temperature glass dynamics. The

experimental data and the theoretical analysis presented here are the first direct evidence that low-temperature glass dynamics occur on fixed local potential surfaces—a fact completely consistent with the TLS model of glasses and incompatible with the other models based on diffusion. The TLS double-well structures should be viewed as an approximate but accurate description of glass potential surface. In fact, the results of temperature-cycling hole-burning measurements agree exactly with the predictions based upon the TLS theory.

VII. Solute–Solvent Effects

It is important to ask whether optical dephasing experiments of the type discussed here probe strictly glass dynamics or a combination of the dye–glass system. Since the magnitude of the coupling between the excited states of the chromophore and the TLS plays a central role in determining the extent of dephasing, comparing the results of any particular technique on different dyes in the same glass will, in general, not give the same dephasing time because of differences in coupling strengths.

It is possible to eliminate the magnitudes of coupling strengths from consideration. Taking the ratio of dephasing times measured by echoes and hole burning divides out the coupling strength. For example, if $P(R) \propto 1/R$ extends from short times to infinitely long times, R_d, the ratio of the dephasing times is[54,55,65,100]

$$R_d = T_2^{*PE}/T_2^{*HB} = [\Theta + \ln (2T_w/T_2)]/\Theta \quad (26)$$

where Θ is a parameter dependent on the specific model of the dynamics. For the uncorrelated sudden jump TLS model used throughout this paper, it is 3.66.[55,64] For any form of $P(R)$, R_d is independent of coupling strength. If dephasing experiments probed glass properties exclusively, R_d will be the same for different chromophores in a particular glass.

It is found from experiments that the R_ds for different chromophores in ethanol glass are similar but not identical.[65] For cresyl violet/ethanol, $R_d = 8.3 \pm 0.3$ at 1.57 K whereas for resorufin/ethanol, $R_d = 5.9 \pm 0.3$. The echo decays of these molecules are exponential. Therefore, $P(R) \propto 1/R$ for fast rates (large R). At long time (small R), $P(R)$ is the log normal distribution obtained from the time-dependent hole-burning experiment shown in Figure 10 for cresyl violet/ethanol as discussed previously. The same long-time results were found in resorufin/ethanol.[68] Therefore the $P(R)$ for slow rates is a property of the bulk glass. The difference between the R_ds for cresyl violet and resorufin is well outside of experimental error and must reflect a difference in the intermediate time scale dynamics.

The difference in R_ds can be due to differences in the local solvent structures around the ion. A realistic view recognizes that solvation shells exist around the ions in the liquid and that the solvation shell will be frozen in when the glass is formed. The solvent shell structures and, therefore, the dynamics are different from those of the bulk glass. When the ion is changed from positive to negative, the bulk dynamics are unchanged but the structure and dynamics of the solvent shell can change. Cresyl violet is a positive ion while resorufin is a negative ion. Therefore the solvent shell structures around these ions will differ. It is interesting to note that the R_d values for rhodamine 640/ethanol and sulforhodamine 640/ethanol are within experimental error of the cresyl violet value. The largest difference is found in going from a positive to a negative ion. The dipolar interaction between the dye and the glass is long range; the electronic states of the dye feel the combined effect of the solvent shell as well as the bulk glass, each with a different rate distribution. The important point is that comparing the R_d values of different ions in the same glass provides a method for examining changes in solvent shell structure and dynamics.

Pack et al. have developed a theory to describe optical line-narrowing experiments in systems with two spatial domains, i.e., a solvent shell close to the chromophore and a bulk glass farther away.[69] Three regimes, related to the concentration of perturbing glass TLS $n(T,T_w)$, the experimental line width, the dipolar coupling strength, D, and the solvation shell radius, r_s, can be identified in a discussion of solvation shell effects. The first may be termed the inner-shell regime. For this situation of all the perturbations yielding the line shape occur within the solvent shell. The conditions fwhm $\gg D/r_s^3$ must hold and perturbations outside the solvent shell radius, r_s, are negligible in comparison to the line width. Invoking the relationship between hole width and $n(T,T_w)$ and D, this implies $n(T,T_w) \gg 1/r_s^2$ must hold. For systems where this is valid, results for different dyes in the same glass will depend on the effect of the individual chromophore on the local structure. The only important distribution of rates will be inside the solvation shell, and the similarity of this to bulk properties will depend on the details of the solvent–chromophore interaction.

A second set of conditions is the outer-shell regime. For a random, low-concentration TLS distribution, few perturbers on average will lie near the chromophore. The back-interaction of a chromophore on the glass will be relatively undetectable in this case. Any effects will be confined to the far wings of the profile. For this to hold, fwhm $\ll D/r_s^3$ and $n(T,T_w) \ll 1/r_s^3$. Perturbations outside the shell are the main contribution to the line width. No significant solvent shell effect will exist under these conditions.

The third case is the intermediate regime in which TLS existing in the solvation shell and the bulk glass both contribute to the line width. When fwhm $\approx D/r_s^3$ and $n(T,T_w) \approx 1/r_s^3$, this intermediate condition holds. Under these conditions, the theory of Pack et al. can calculate the hole-burning line shape, and both the solvent shell and the bulk contribute significantly to the line profile. Physically plausible values of the active TLS concentration, $n(T,T_w) = 7.0 \times 10^{-4}$(TLS)/Å^3, and dipolar coupling strength, $D = 2.73 \times 10^{12}$ Hz Å^3, are used for the calculations. For uniform spatial distribution of TLS, this yields a Lorentzian line width of 4.00 GHz. From Stark experiments the change in dipole moment between ground and excited states for ionic dyes is known to be on the order of $\Delta\mu_M = 1$ D.[101] Using the conversion factor of (1 D)$^2 = 1 \times 10^{36}$ erg/cm^3 $= 1.509 \times 10^{14}$ Hz/Å^3, one finds the change in dipole moment of the tunneling systems would be on the order of $\Delta\mu_{TLS} = 0.02$ D for the choice of coupling parameter, D, used.

The effect of altering the local dynamics is investigated by lowering the value of $n(T,T_w)$ inside the sol-

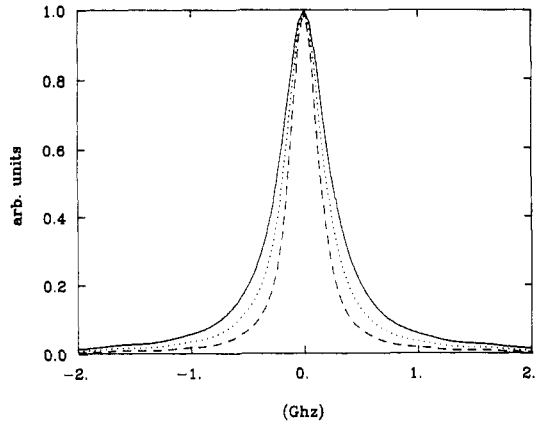

Figure 13. Hole shapes calculated for a system with solvent shells around the chromophores. The solvent shell has a different structure and, therefore, different dynamics than the bulk glass. The chromophores interact with both the solvent shell and the bulk glass through the long-range dipolar coupling. The solvent shell has a radius of 20 Å and has a different rate distribution than the bulk. As a model of the solvent shell, the concentration of TLS in the shell is reduced. The dotted and dashed lines are model calculations with, respectively, 25% and 50% of the TLS in the solvent shell frozen. The hole contracts but remains Lorentzian.

vation shell. Such a reduction might occur if an ordering of local solvent dipolar molecules around an ionic chromophore led to a lower concentration of TLS. It is known from hole-burning experiments on resorufin/ethanol[82] that, after a bulk transition from the amorphous phase to the plastic crystalline phase, the dynamics are reduced by a factor of 10, most likely due to a reduction in $n(T,T_w)$. The plastic crystal phase is orientationally disordered but somewhat ordered translationally. A postulated back-reaction of the chromophore on the solvent might induce some similar local ordering. Similar reductions could be obtained if the chromophore, through electrostatic or bonding effects, increased TLS potential barriers slowing some of the tunneling processes out of the experimental time scale.

The calculations show that it is still possible to obtain holes that are experimentally indistinguishable from Lorentzian even though there are two spatial domains. Figure 13 shows plots of holes calculated by assuming the local solvent shell/bulk glass picture. As the concentration of TLS in the solvent shell is reduced, the hole narrows but remains essentially Lorentzian. Only very large perturbations of the local dynamics will give rise to a hole shape that is distinguishably non-Lorentzian. Therefore the observation of an apparently Lorentzian hole cannot rule out solvation shell effects. We conclude that significant alteration of local glass dynamics could occur without the effect manifesting itself in measurements taken on a single time scale on a single dye molecule. Examining R_d for several molecules in the same glass can reveal solvent shell effects.

A change of the order of 30% in the local dynamics is necessary to cause the variation of R_d values observed between resorufin and other dyes investigated. Resorufin is the only anionic dye studied so far. To learn if there is a systematic dependence on chromophore charge, measurements of other anions would be useful. Mapping out more of the distribution of rates with a combination of experimental techniques should provide further insight into solute ion dependent properties in ethanol glasses and on what time scale these solute–solvent effects are manifested.

VIII. Conclusions

We have presented the results of optical dephasing measurements on glassy systems that operate on different time scales as well as a framework for consistently interpreting the results. It is possible to exploit the different time sensitivities of various dephasing techniques to quantitatively measure important dynamical quantities such as fluctuation rate distributions. Temperature-dependent echo and hole-burning data show characteristics ascribable to TLS behavior at low temperatures but are affected by non-TLS, exponentially activated processes at higher temperature. Lorentzian holes and exponential decays show that the dye–glass coupling must be dipolar, and exponential echo decays further require that the fluctuation rate distribution $P(R)$ goes as $1/R$ at short times (fast rates). Time-dependent hole-burning data demonstrate that a log normal distribution occurs in ethanol glass for slow rates (long times).

The experiments have been able to verify the fixed potential surface postulate of the TLS model by temperature-cycled hole burning in which reversible hole broadening excludes defect diffusion and other models based on time-evolving local surfaces. Another benefit to combining measurements done over several orders of magnitude in time is the ability to infer properties about solute–solvent interactions in complex systems which would not be possible with any single type of measurement. There are still many questions remaining to be answered. Among these are the fluctuation rate distributions at intermediate (nanoseconds to milliseconds) times. Furthermore, although TLS are remarkably successful in accounting for observed behaviors, no one has identified what a TLS is. Optical dephasing techniques will continue to be an important tool for developing a better understanding of glasses and other complex materials.

In addition to being probes of dynamics, the techniques mentioned here are being studied for practical methods for the optical storage of information at very high densities.[45-47] The ability to burn many relatively narrow holes in a broad inhomogeneous distribution immediately brings up the possibility of encoding binary data by the presence or absence of a hole in the spectrum. A great deal of effort is being expended in developing materials that can be burned (set) and read quickly as well as being able to be filled (reset). A detailed understanding of how glasses evolve in time is an essential component in searching for materials that fit these requirements.

IX. Acknowledgments

We thank Dr. C. A. Walsh and Prof. Mark Berg for their contributions to this work. This work was supported by the National Science Foundation Division of Materials Research (Grant DMR87-18959) and the Office of Naval Research Physics Division (Contracts N00014-89-J1119 and N00014-89-K0154). L.R.N. and K.A.L. thank the Fannie and John Hertz Foundation and AT&T Bell Laboratories, respectively, for graduate fellowships. A.E. thanks the Deutsche Forschungsge-

meinschaft for a postdoctoral fellowship.

X. Appendix

In this appendix it is demonstrated that a diffusion-based model predicts an irreversible hole width in temperature cycle experiments even at low temperatures. It has been shown that in the limit of slow fluctuations the four-point correlation function for a large number of independent perturbers is[55]

$$C(\tau,T_w,\tau) = \exp\{-N\langle 1 - \exp(i\phi(\tau,T_w))\rangle\}$$

$$\phi(\tau,T_w) = \tau[\Delta\omega(0) - \Delta\omega(T_w)] \qquad \text{(A.1)}$$

where $\langle\ \rangle$ denotes an average over all the coordinates of the glass and $\Delta\omega(t)$ is the frequency shift caused by a single perturber. The limit of slow fluctuations implies that $\Delta\omega(t)$ does not vary during the intervals $(0,\tau)$ and $(T_w+\tau,T_w+2\tau)$.

The relevant coordinates in the case of diffusive motion are the initial positions of the perturbers and their relative positions at time T_w. $\Delta\omega(0)$ and $\Delta\omega(T_w)$ may be expressed as functions of these coordinates. $\Delta\omega(0) = \Delta\omega(r)$ and $\Delta\omega(T_w) = \Delta\omega(\vec{r} + \vec{r}_d)$, where $\vec{r}$ is the initial perturber position and $\vec{r}_d$ is the position of the perturber at time T_w relative to its initial location. With this in mind, eq A.1 becomes

$$C(\tau,T_w,\tau) = \exp\{-N\langle 1 - \exp(i\phi(\vec{r},\vec{r}_d))\rangle_{\vec{r},\vec{r}_d}\}$$

$$\phi(\vec{r},\vec{r}_d) = \tau[\Delta\omega(\vec{r}) - \Delta\omega(\vec{r} + \vec{r}_d)] \qquad \text{(A.2)}$$

If the $\vec{r}$ and $\vec{r}_d$ distributions have no angular dependence and the function $\Delta\omega(\vec{r})$ is also dependent only upon the magnitude of its argument, the imaginary terms in eq A.2 vanish when the averages over $\vec{r}$ and $\vec{r}_d$ are performed. Thus the correlation function becomes

$$C(\tau,T_w,\tau) = \exp\{-N\langle 1 - \cos\ (\phi(\vec{r},\vec{r}_d))\rangle_{\vec{r},\vec{r}_d}\} \qquad \text{(A.3)}$$

which, when converted to integral form, is

$$C(\tau,T_w,\tau) = \exp\left\{-2N\int \sin^2\ [\phi(\vec{r},\vec{r}_d)/2]P(\vec{r})P(\vec{r}_d,T_w)\ d\vec{r}\ d\vec{r}_d\right\}$$

$$\phi(\vec{r},\vec{r}_d) = [\Delta\omega(\vec{r}) - \Delta\omega(\vec{r} + \vec{r}_d)]\tau \qquad \text{(A.4)}$$

The accumulated phase error, $\phi(\vec{r},\vec{r}_d)$, is assumed to be monotonically related to $|r_d|$; that is, $\phi(\vec{r},\vec{r}_d)$ increases as $|r_d|$ increases. For the sake of simplicity, the distribution of final perturber positions is assumed to be Gaussian and independent of $\vec{r}$. In the simple fixed-temperature case, $P(\vec{r}_d,T_w)$ is $P(\vec{r}_d,T_w) \propto \exp(-|r_d|^2/(4DT_w)^{-1})$, where D is a diffusion constant. D is a function of temperature and the relevant internal parameters responsible for diffusion. The form of $D(T)$ is unimportant. When the temperature cycle is considered, the form of the $P(\vec{r}_d,T_w)$ distribution, eq A.4, is modified. Taking the temperature cycle to be described as a step function, i.e.

$$T(t) = T_0 \qquad t \le t_1 \qquad \text{(A.5a)}$$

$$T(t) = T_1 \qquad t_1 \le t \le t_2 \qquad \text{(A.5b)}$$

$$T(t) = T_0 \qquad t > t_2 \qquad \text{(A.5c)}$$

one may show that $P(\vec{r}_d,T_w)$ during the temperature cycle is described by

$$P(\vec{r}_d,T_w) \propto \exp\{-|r_d|^2[4D_0T_w]^{-1}\} \qquad T_w \le t_1 \qquad \text{(A.6a)}$$

$$P(\vec{r}_d,T_w) \propto \exp\{-|r_d|^2[4(D_0t_1 + D_1(T_w - t_1))]^{-1}\} \qquad t_1 \le T_w \le t_2 \qquad \text{(A.6b)}$$

$$P(\vec{r}_d,T_w) \propto \exp\{-|r_d|^2[4(D_0t_1 + D_1(t_2 - t_1) + D_0(T_w - t_2))]^{-1}\} \qquad T_w > t_2 \qquad \text{(A.6c)}$$

where D_0 and D_1 are the diffusion constants at the low and high temperatures, respectively. The key feature of eq A.6 is that it is a Gaussian of monotonically increasing half-width. Recall that the correlation function, eq A.3, is directly related to the hole width (rate of decay in an echo experiment).[54,100] By increasing the width of the $P(\vec{r}_d,T_w)$ distribution, the averages in eq 16 are weighted toward larger accumulated phase errors. This leads directly to a faster decaying $C(\tau,T_w,\tau)$ which, when converted to frequency, is equivalent to a broader line width. Thus it may be concluded that, in a diffusive model, the line width broadens constantly. Cycling the temperature only forces the line width to evolve at a different rate at the higher temperature. When the temperature is again lowered, the line does not narrow but merely continues to broaden at the original rate. This is clearly in direct contradiction to the experimental evidence of a reversible line width as is documented in Figure 12. Therefore it may be concluded that a diffusive model is not valid in these systems.

XI. References

(1) *Amorphous Solids: Low Temperature Properties*; Phillips, W. A., Ed.; Springer: New York, 1981.
(2) Finegold, L.; Phillips, N. E. *Phys. Rev.* **1969**, *177*, 1383.
(3) Jackson, H. E.; Walker, C. T.; McNelly, T. F. *Phys. Rev. Lett.* **1970**, *25*, 26.
(4) Kittel, C. *Introduction to Solid State Physics*, 5th ed.; Wiley: New York, 1976; Chapters 4–6.
(5) Stephens, R. B. *Phys. Rev. B* **1973**, *8*, 289.
(6) Kelham, S.; Rosenberg, H. M. *J. Phys. C.* **1981**, *14*, 1737.
(7) Zeller, R. C.; Pohl, R. O. *Phys. Rev. B* **1971**, *4*, 2029.
(8) Lasjaunias, J. C.; Ravex, A.; Vandorpe, M. *Solid State Commun.* **1975**, *17*, 1045.
(9) Anderson, A. C.; Reese, W.; Wheatley, J. C. *Rev. Sci. Instrum.* **1963**, *34*, 1386.
(10) Mahle, S. M.; McCammon, R. D. *Phys. Chem. Glasses* **1969**, *10*, 222.
(11) von Schickfus, M.; Hunklinger, S. *Phys. Lett.* **1977**, *64A*, 144.
(12) Alben, J. O.; Beece, D.; Bowne, S. F.; Doster, W.; Eisenstein, L.; Frauenfelder, H. O.; Good, D.; McDonald, J. D.; Marden, M. C.; Moh, P.; Reinisch, L.; Reynolds, A. H.; Shyamsunder, E.; Yue, K. T. *Proc. Natl. Acad. Sci. U.S.A.* **1982**, *79*, 3744.
(13) Macfarlane, R. M.; Shelby, R. M. *J. Lumin.* **1987**, *36*, 179.
(14) Rebane, K. K.; Rebane, L. A. In *Persistent Spectral Hole-Burning: Science and Applications*; Moerner, W. E., Ed.; Springer-Verlag: Berlin, 1988; Chapter 2.
(15) Hayes, J. M.; Jankowiak, R.; Small, G. J. *Persistent Spectral Hole-Burning: Science and Applications*; Moerner, W. E., Ed.; Springer-Verlag: Berlin, 1988.
(16) diBartolo, B. *Optical Interactions in Solids*; Wiley: New York, 1968.
(17) Golding, B.; Graebner, J. *Amorphous Solids: Low Temperature Properties*; Phillips, W. A., Ed.; Springer: New York, 1981.
(18) Goubau, W. M.; Tait, R. H. *Phys. Rev. Lett.* **1975**, *34*, 1220.
(19) Black, J. L.; Halperin, B. I. *Phys. Rev. B* **1977**, *16*, 2879.
(20) Breinl, W.; Friedrich, J.; Haarer, D. *J. Chem. Phys.* **1984**, *81*, 3915.
(21) Skinner, J. L. *J. Chem. Phys.* **1982**, *77*, 3398.
(22) Pohl, R. O. *Amorphous Solids: Low Temperature Properties*; Phillips, W. A., Ed.; Springer: New York, 1981; Chapter 3.
(23) Lewis, J. E.; Lasjaunias, J. C.; Shumacher, G. *J. Phys. (Paris)* **1978**, *39*, Suppl. C6-967.
(24) Loponen, M. J.; Dynes, R. C.; Narayanamurti, V.; Garno, J. P. *Phys. Rev. Lett.* **1980**, *45*, 457.
(25) Hunklinger, S.; von Schickfus, M. *Amorphous Solids; Low Temperature Properties*; Phillips, W. A., Ed.; Springer: New York, 1981; Chapter 6.
(26) Walton, D. *Solid State Commun.* **1974**, *14*, 335.

(27) Redfield, D. *Phys. Rev. Lett.* **1971**, *27*, 730.
(28) Tanttilla, W. H. *Phys. Rev. B* **1977**, *39*, 554.
(29) Anderson, P. W.; Halperin, B. I.; Varma, C. M. *Philos. Mag.* **1972**, *25*, 1.
(30) Phillips, W. A. *J. Low Temp. Phys.* **1972**, *7*, 351.
(31) Huber, D. L.; Broer, M. M.; Golding, B. *Phys. Rev. Lett.* **1984**, *52*, 2281.
(32) Yu, C.; Leggett, A. *Comments Condens. Matter Phys.* **1988**, *14*, 231.
(33) Weber, M. J. *J. Lumin.* **1987**, *36*, iii.
(34) Moerner, W. E.; Lenth, W.; Bjorklund, G. C. *Persistent Spectral Hole-Burning: Science and Applications*; Moerner, W. E., Ed.; Springer-Verlag: Berlin, 1988; Chapter 7.
(35) Personov, R. I.; Al'Shits, E. I.; Bykovskaya, L. A. *Opt. Commun.* **1972**, *6*, 169.
(36) Gorokhovskii, A. A.; Kaarli, R. K.; Rebane, L. A. *JETP Lett.* **1974**, *20*, 216.
(37) Hartmann, S. R. *Sci. Am.* **1968**, *128*, 32.
(38) Szabo, A. *Phys. Rev. Lett.* **1970**, *25*, 924.
(39) Kharlamov, B. M.; Personov, R. I.; Bykovskaya, L. A. *Opt. Commun.* **1974**, *12*, 191.
(40) Jankowiak, R.; Small, G. J. *Science* **1987**, *237*, 618.
(41) Jäckle, J.; Jüngst, K.-L. *Z. Phys. B* **1978**, *30*, 243.
(42) Elschner, A.; Richert, R.; Bässler, H. *Chem. Phys. Lett.* **1986**, *127*, 105.
(43) Jankowiak, R.; Shu, L.; Kenney, M. J.; Small, G. J. *J. Lumin.* **1987**, *36*, 293.
(44) van den Berg, R. H.; Völker, S. V. *Chem. Phys.* **1988**, *128*, 257.
(45) Lee, H. W. H.; Gehrtz, M.; Marinero, E.; Moerner, W. E. *Chem. Phys. Lett.* **1985**, *118*, 611.
(46) Wild, U. P.; Bucher, S. E.; Burkhalter, F. A. *Appl. Opt.* **1985**, *24*, 1526.
(47) Bai, Y. S.; Babbitt, W. R.; Mossberg, T. W. *Opt. Lett.* **1984**, *11*, 724.
(48) Shelby, R. M.; Macfarlane, R. M. *J. Lumin.* **1984**, *31 & 32*, 839.
(49) Bai, Y. S.; Fayer, M. D. *Commun. Condens. Matter Phys.* **1989**, *14*, 343.
(50) Schulte, G.; Grond, W.; Haarer, D.; Silbey, R. *J. Chem. Phys.* **1988**, *88*, 679.
(51) Kubo, R. In *Fluctuation, Relaxation, and Resonance in Magnetic Systems. Proceedings of the Scottish University's Summer School*; ter Haar, D., Ed.; Oliver and Boyd: London, 1961.
(52) Mukamel, S. *Phys. Rev. A* **1983**, *28*, 3480. Mukamel, S. *Phys. Rep.* **1982**, *93*, 1.
(53) Loring, R. F.; Mukamel, S. **1985**, *83*, 2116. Loring, R. F.; Yan, Y. J.; Mukamel, S. *J. Chem. Phys.* **1987**, *87*, 5840. Mukamel, S.; Loring, R. F. *J. Opt. Soc. Am. B* **1986**, *3*, 595.
(54) Berg, M.; Walsh, C. A.; Narasimhan, L. R.; Littau, K. A.; Fayer, M. D. *J. Chem. Phys.* **1988**, *88*, 1564.
(55) Bai, Y. S.; Fayer, M. D. *Phys. Rev. B* **1989**, *39*, 11066.
(56) Abella, I.; Kurnit, N. A.; Hartmann, S. R. *Phys. Rev.* **1966**, *141*, 391.
(57) Walsh, C. A.; Berg, M.; Narasimhan, L. R.; Fayer, M. D. *Acc. Chem. Res.* **1987**, *20*, 120.
(58) Rebane, K. K.; Gorokhovskii, A. A. *J. Lumin.* **1987**, *36*, 237.
(59) Small, G. J. In *Spectroscopy and Excitation Dynamics of Condensed Molecular Systems*; Agranovich, V. M., Hochstrasser, R. M., Eds.; North-Holland: Amsterdam, 1981; Chapter 9.
(60) Walsh, C. A.; Berg, M.; Narasimhan, L. R.; Fayer, M. D. *J. Chem. Phys.* **1987**, *86*, 77.
(61) Rebane, A.; Haarer, D. *Chem. Phys. Lett.* **1989**, *70*, 478.
(62) Brocklesby, W. S.; Golding, B.; Simpson, J. R. *J. Lumin.*, in press.
(63) Fidder, H.; DeBoer, S.; Wiersma, D. *Chem. Phys.* **1989**, *139*, 317. Saikan, S.; Nakabayashi, T.; Kanematsu, Y.; Tato, N. *Phys. Rev. B* **1988**, *38*, 7777.
(64) Maynard, R.; Rammal, R.; Suchail, R. *J. Phys. (Paris), Lett.* **1980**, *41*, L291. Note that there is an error in a numerical integral in this reference. The value reported as 2.63 should be 3.66.
(65) Narasimhan, L. R.; Pack, D. W.; Fayer, M. D. *Chem. Phys. Lett.* **1988**, *152*, 287.
(66) Elschner, A.; Narasimhan, L. R.; Fayer, M. D. *Chem. Phys. Lett.*, submitted for publication, 1990.
(67) Thijssen, H. P. H.; van den Berg, R.; Völker, S. *Chem. Phys. Lett.* **1983**, *103*, 23.
(68) Littau, K. A.; Bai, Y. S.; Fayer, M. D. *Chem. Phys. Lett.* **1989**, *159*, 1. Littau, K. A.; Bai, Y. S.; Fayer, M. D. *J. Chem. Phys.*, accepted.
(69) Pack, D. W.; Narasimhan, L. R.; Fayer, M. D. *J. Chem. Phys.*, accepted.
(70) Putikka, W. O.; Huber, D. L. *Phys. Rev. B* **1987**, *36*, 3436.
(71) Aartsma, T. J.; Morsink, J.; Wiersma, D. *Chem. Phys. Lett.* **1977**, *47*, 425. Hesselink, W. H.; Wiersma, D. A. *Spectroscopy and Excitation Dynamics of Condensed Molecular Systems*; Agranovich, V. M., Hochstrasser, R. M., Eds.; North-Holland: Amsterdam, 1981; Chapter 6. Olson, R. W.; Meth, J. S.; Marshall, C. D.; Newell, V. J.; Fayer, M. D. *J. Chem. Phys.*, accepted.
(72) Sturge, M. D.; McCumber, D. E. *J. Appl. Phys.* **1963**, *34*, 1682.
(73) Hahn, E. L. *Phys. Rev.* **1950**, *80*, 580.
(74) Slichter, C. P. *Principles of Magnetic Resonance*; Springer: Berlin, 1978.
(75) Abragam, A. *Nuclear Magnetism*; Clarendon: Oxford, 1982.
(76) Völker, S.; Macfarlane, R. M.; Genack, A. Z.; Trommsdorff, H. P.; van der Waals, J. H. *J. Chem. Phys.* **1977**, *67*, 1759.
(77) Lyo, S. K.; Orbach, R. *Phys. Rev. B* **1980**, *22*, 4223.
(78) Boyd, R. W.; Mukamel, S. *Phys. Rev. A* **1984**, *29*, 1973.
(79) Thijssen, H. P. H.; Völker, S. *Chem. Phys. Lett.* **1985**, *120*, 496.
(80) Thijssen, H. P. H.; van den Berg, R.; Völker, S. *J. Phys. (Paris)* **1985**, C7-363.
(81) Haida, O.; Suga, H.; Seki, J. *J. Chem. Thermodyn.* **1977**, *9*, 1113.
(82) van den Berg, R.; Völker, S. *Chem. Phys. Lett.* **1987**, *137*, 201.
(83) Littau, K. A., unpublished results.
(84) Hu, P.; Walker, L. R. *Phys. Rev. B* **1978**, *18*, 1300.
(85) Lasjaunias, J. C.; Maynard, R.; Vandorpe, M. *J. Phys. (Paris)* **1978**, Suppl. C6-973.
(86) Hesselink, W. H.; Wiersma, D. A. *J. Chem. Phys.* **1980**, *73*, 648.
(87) Jackson, B.; Silbey, R. *Chem. Phys. Lett.* **1983**, *99*, 331.
(88) Jankowiak, R.; Bässler, H.; Silbey, R. *Chem. Phys. Lett.* **1986**, *125*, 139.
(89) Lee, H. W. H.; Patterson, F. G.; Olson, R. W.; Wiersma, D. A.; Fayer, M. D. *Chem. Phys. Lett.* **1982**, *90*, 172.
(90) Kokai, F.; Tanaka, H.; Brauman, J. I.; Fayer, M. D. *Chem. Phys. Lett.* **1988**, *143*, 1.
(91) Jankowiak, R.; Small, G. J.; Ries, B. *Chem. Phys.* **1987**, *118*, 223.
(92) Littau, K. A.; Elschner, A. E.; Fayer, M. D. *Chem. Phys. Lett.*, in preparation.
(93) van den Berg, R.; Visser, A.; Völker, S. *Chem. Phys. Lett.* **1988**, *144*, 105.
(94) Friedrich, J.; Haarer, D. *Angew. Chem.* **1984**, *23*, 113.
(95) Köhler, W.; Zöllfrank, J.; Friedrich, J. *Phys. Rev. B* **1989**, *39*, 5414.
(96) Bai, Y. S.; Littau, K. A.; Fayer, M. D. *Chem. Phys. Lett.* **1989**, *162*, 449.
(97) Klauder, J. R.; Anderson, P. W. *Phys. Rev.* **1962**, *125*, 912.
(98) Mims, W. B. *Phys. Rev.* **1968**, *168*, 370.
(99) Sievers, A. J.; Takeno, S. *Phys. Rev. B* **1989**, *39*, 3374.
(100) Bai, Y. S.; Fayer, M. D. *Chem. Phys.* **1988**, *128*, 135.
(101) Renn, A.; Bucher, S. E.; Meixner, A. J.; Meister, E. C.; Wild, U. P. *J. Lumin.* **1988**, *39*, 181.